Resilient Microgrid Planning for Socially Vulnerable Communities

Farzane Ezzati[1], Zhijie Sasha Dong[2], Gino Lim[3], and Junfeng Jiao[4]

[1]University of Houston, USA , fezzati@cougarnet.uh.edu
[2]Southeast University, China , sasha@seu.edu.cn
[3]University of Houston, USA , ginolim@central.uh.edu
[4]The University of Texas at Austin, USA , jjiao@austin.utexas.edu

Abstract

Climate change has increased the frequency and severity of natural disasters, disrupting power systems and disproportionately impacting socially vulnerable communities. While recent research has explored technical and socio-economic aspects of microgrid deployment, there remain limited work on designing microgrids that specifically enhance energy resilience for socially vulnerable communities during disasters. To address this gap, this study proposes an investment and resilience-oriented framework for planning and operation of renewable energy-integrated Residential Community Microgrid (RCMG). A two-stage stochastic programming model is developed to optimize long-term investment, operation, and capacity expansion under uncertainties in load demand, renewable generation, and outage duration. The framework also incorporates a load-curtailing demand response program (DRP) that incentivizes households through bill discounts. Results from case studies in three Texas communities demonstrate that integrating capacity expansion with DRP can reduce total system costs by up to 16% while improving resilience by more than 60% and increasing household bill savings by 13%. The findings highlight the critical roles of DRP design, expansion timing, and differentiated electricity pricing in balancing financial accessibility and resilience. Scalability analysis shows that while expansion costs scale with demand, investment responses are shaped by social vulnerability, highlighting the need for proactive, community-specific planning and front-loaded funding to ensure equitable microgrid growth. These insights provide practical guidance for utilities and policymakers in planning equitable, community-specific microgrids that strengthen energy resilience under growing climate risks.

Keywords: Climate Change; Microgrids; Social Vulnerability; Resilience; Stochastic Programming.

1 Introduction

In recent years, power systems have shown significant vulnerability to climate disasters. According to the most recent data from the National Energy Technology Laboratory (NETL) [1], 2,440 power outages were occurred in the U.S. between 2015 and 2023. Of these, 878 outages (36.0%) were caused by severe weather, and 61% lasted at least six hours. Notable examples include: i) Winter Storm Uri (February 2021), which struck the U.S., particularly Texas, causing natural gas system failures and a near-total grid collapse. The resulting supply–demand imbalance led to prolonged load shedding, leaving millions of Texans without power for up to five days and 246 deaths from extreme cold. ii) Hurricane Beryl (July 2024), which swept through southeast Texas, caused widespread power system damage and left nearly 2.3 million customers without electricity for several days. About one-third of the storm-related deaths were due to heat exposure.

A four-year NETL analysis shows a 90.62% increase in the U.S. weather-related power outages from 2020–2023 compared to 2016–2019, a trend largely driven by climate change, which has led to more intense rainfall, heatwaves, and storms. Texas consistently experiences the highest number of weather-related outages nationwide, with 210 major events from 2000–2023 and 263 outages in just 2019–2023, far surpassing other states [2, 3]. Given the rising frequency of natural disasters and their severe impacts on the power systems, strengthening their resilience has become a critical priority in the U.S.

In response, various strategies have been proposed to enhance power systems resilience, including system hardening and operational improvements [4–6]. Among these, microgrids (MGs) stand out as one of the most promising solutions [7]. The U.S. Department of Energy defines a MG as a group of interconnected loads and distributed energy resources (DER) within clearly defined electrical boundaries that acts as a single controllable entity with respect to the grid. MGs can function in both grid-connected and islanded modes [8], supporting energy resilience by maintaining power supply during grid outages and supporting critical infrastructure. MGs integrating DERs with advanced strategies are key enablers of resilient future grids [9].

In recent years, there have been significant advancements in the planning and operation of MGs, driven mainly by three factors: increasing incorporation of renewable energy sources (RES), the need for grid flexibility, and the growing complexity of MG operations [10]. The key advancements

include intelligent energy management systems (EMS), advanced energy storage system (ESS) management, transactive energy (TE), and cyber-physical security, which are primarily designed to further improve performance, reliability, efficiency, and resilience of power systems.

Although MGs offer significant potential, uncertainties in renewable generation, demand, and compensation market, high costs, application-specific constraints, and complex operational requirements pose challenges to realizing their full benefits [11]. Hence, strategies such as proactive management, optimal placement/scheduling, and operation strategies have been proposed [7]. Moreover, the introduction of Demand Response Programs (DRPs) has further emphasized the development of price- and incentive-based strategies aimed at reducing investment costs, increasing revenue, lowering electricity bills, and improving system reliability and resilience [12–14]. While current strategies provide valuable solutions, the application of MGs across different sectors requires tailored implementation and analysis to develop effective planning and scheduling mechanisms.

Building on these operational and economic considerations, recent studies have also emphasized the importance of expanding MG deployment to meet evolving grid demands. As the demand for flexible, low-carbon, and resilient power systems grows, expanding MG deployment has become a central focus in the literature. Studies highlight the importance of scalable planning frameworks that address both technical and socio-economic challenges of MG expansion [15]. These efforts are essential for meeting increasing energy demands, accommodating renewable integration, and supporting system-wide resilience.

While recent research has increasingly focused on these challenges, optimizing MGs for socially vulnerable communities and achieving equity remains an open area of inquiry [16–18]. Social vulnerability (SV), which determines the extent to which individuals' lives and possessions are at risk due to limited adaptive capacity [19], has been defined across many disasters and is increasingly studied in the context of prolonged power outages [20, 21]. Willingness-to-pay (WTP), on the other hand, quantifies how households value reliable electricity, providing an economic perspective on resilience investments [22]. Both factors are critical for MG operations: SV influences communities' recovery from outages and WTP guides investment, pricing, and equitable allocation of resilience benefits. Integrating such socio-economic considerations alongside technical capabilities ensures that MG deployment and operation effectively supports resilient and equitable electricity supply [23, 24].

These socio-technical factors highlight critical issues that require further analysis, motivating the central research question of this study: **How are costs, energy resilience, and equity in socially vulnerable community MGs influenced by expansion timing, demand response program settings, electricity pricing, and community scale?**

To address this question, this study proposes an investment- and resilience-oriented framework for planning and operating renewable energy–integrated Residential Community Microgrids (RCMG). A two-stage mixed-integer stochastic programming model is developed to minimize investment, expansion, and operational costs under uncertainties in demand, power generation, and outage duration. The first stage determines optimal locations and capacities of devices, while the second handles capacity expansion and scheduling. An incentivized DRP is incorporated that encourages load curtailing during off-peak hours to support system balance and consumer convenience during peak-hours. The model is solved using a Benders Decomposition combined with Branch & Bound algorithm. The study contributes to the literature as follows:

- First, our model advances renewable MG planning by integrating resilience and DRP under uncertainty, addressing key challenges in achieving reliable and sustainable residential energy systems. It contributes to ongoing efforts in MG optimization and consumer-oriented strategies that support grid flexibility and cost-effectiveness.

- Second, the study examines long-term MG planning for socially vulnerable communities. Our framework evaluates SV effects on both financial outcomes and resilience, supporting informed decision-making.

- Third, this paper explores the role of a curtail-based DRP in influencing energy resilience and investment strategies, offering insights into operational efficiency and sustainability. Application to three residential communities with varying SV provides practical insights, and the sensitivity analysis identifies tailored strategies for investment, operation, and pricing.

The remainder of the paper is organized as follows. Section (2) provides a literature review. Section (3) formalizes the RCMG and Section (4) provides the developed energy resilience metrics. Section (5) presents the real case studies, along with data collection process. Section (6) offers a systematic numerical analysis on the outputs of the model. The discussion on operation and managerial implications is provided in Section (7) and the study is concluded in Section (8).

2 Literature Review

A community microgrid designed for residential use is a system comprising of DER (either renewable or fossil-based), ESS, EMS, and households as the consumers. Existing literature has examined MGs under various assumptions with different considerations of current challenges. Here we provide a review on the literature in two categories and highlight the importance of our study in each.

2.1 MG Investment & Expansion under Uncertainty

MG investment and expansion planning are fundamentally challenged by uncertainties that impact both short-term operations and long-term decisions, most notably the duration of power outages, fluctuating load demand, and renewable energy generation [13, 25–28]. Furthermore, evolving consumption patterns require planners to forecast not only current but also future load profiles, taking into account both the stochastic nature of power demand and the influence of DER integration and demand-side management [29].

Stochastic programming has emerged as a primary method for addressing these uncertainties in MG planning and scheduling optimization [13, 26–28]. Most contemporary frameworks use two-stage or multi-stage stochastic models to capture uncertainties associated with DER availability, outage durations, and market prices, typically optimizing scheduling and expansion plans to maximize economic benefits and enhance reliability [13, 26–28]. However, many studies only address uncertainties in isolation (e.g., outage duration or load fluctuations), resulting in frameworks that lack completeness when multiple uncertainties co-occur (e.g. [30–32]. A comprehensive approach that jointly considers all major uncertainties (power outage duration, load demand variation, and long-term load growth) remains sparsely addressed in the literature, revealing a research gap around integrated, multi-factor optimization under uncertainty.

The long-term growth of load demand significantly affects expansion decisions in microgrid planning since underestimating growth can result in insufficient capacity, and overestimating increases unnecessary investment. While there is adequate expansion studies with fixed demand growth [33–37], recent research explicitly incorporates load demand growth scenarios into the expansion planning stage using stochastic or robust optimization, enhancing solution resilience to unpredictable demand evolution [34, 38, 39]. These studies demonstrate that strategies ignoring

demand growth risk both economic inefficiency and reduced service reliability over time. Despite advances, few approaches holistically integrate demand growth models with outage and operational uncertainties in a unified investment and scheduling framework, indicating an important area for future research.

In summary, while significant progress has been made in addressing uncertainties in microgrid expansion using stochastic programming, most existing models only partially capture the combined effects of power outage duration, evolving load demand, and demand growth over the planning horizon. The design and application of a comprehensive, unified optimization framework to systematically consider all key uncertainties concurrently remain a critical and underexplored research frontier.

2.2 Demand Response in MG Planning & Scheduling

DRPs are pivotal in supporting microgrid efficiency by enabling consumers to adjust their electricity usage in response to price signals or incentives. In the context of microgrid optimization, DRPs also play an important role in mitigating uncertainties associated with renewable energy sources, market price fluctuations, and variable load demands [26].

Recent trends reveal a shift toward integrating DRP into MG planning and scheduling using increasingly diverse and dynamic strategies. Studies emphasizes the adoption of load shifting [40, 41], real-time pricing [42, 43], and time-of-use pricing [44, 45] to enhance MG flexibility, operational efficiency, and resilience. Modern optimization frameworks favor hybrid stochastic approaches to balance profit, risk, and service continuity, especially under uncertainty and potential islanding events [46]. There is a move toward incentive-driven and event-based DRPs, which allow MGs to dynamically respond to price signals or system emergencies, and these approaches now frequently utilize advanced metaheuristics or multi-level models to maximize social welfare and grid stability [47–49]. Furthermore, joint MG investment and operation increasingly use DRP for both short-term peak shaving and long-term risk management, highlighting its role in integrated energy systems.

Despite these advances, literature recognizes ongoing challenges and research gaps, most notably the need to better address investment impacts and resilience, particularly in contexts affected by evolving load patterns, decentralized generation, and social equity concerns [50].

3 RCMG

The proposed RCMG, Figure (1), comprises battery ES systems, photovoltaics (PV), diesel generators (DG), all managed by a centralized Energy Management System (EMS), and households serving as consumers. The EMS is a combination of hardware and software tools that optimizes energy generation, storage, and consumption. It should be noted that the RCMG is presented as a theoretical framework, and detailed component dynamics (e.g., EMS, PV, and ES) are not modeled explicitly, as the focus is on system-level analysis of cost, resilience, and equity. Under normal conditions, the RCMG operates alongside the main grid, but during outages it becomes islanded and relies on local energy resources. EMS, as the control center, manages devices, the allocation of power to households, and DRP dynamics.

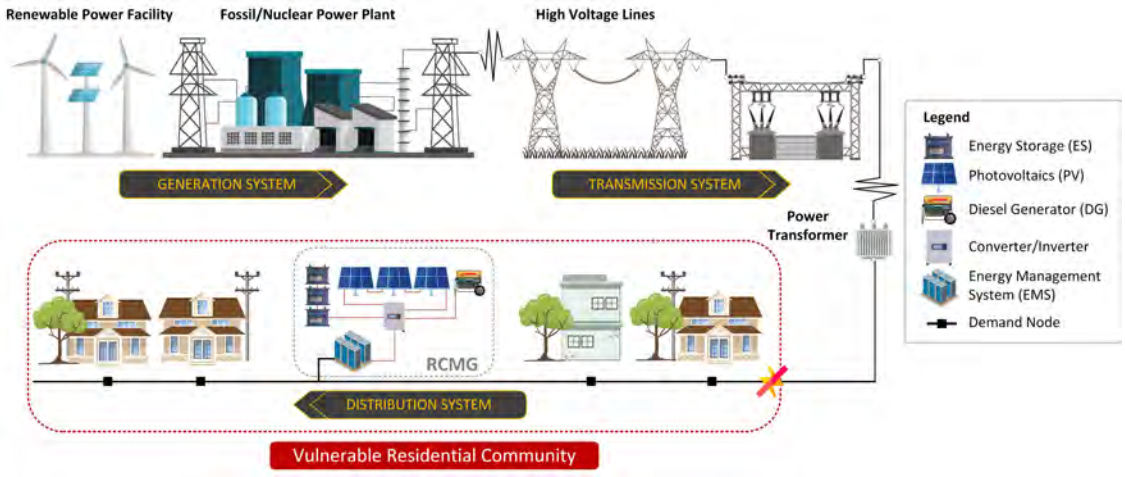

Figure 1: The outline of the RCMG and its position in the power systems.

We consider a load-curtailing DRP for the RCMG to enhance resilience during power outages by enabling immediate demand reduction during high-impact or extended outages without complex scheduling or high consumer flexibility. The DRP shifts the load demand from peak to off-peak hours to conserve energy for critical periods, especially during outages. Figure (2) illustrates this mechanism. Consumers who voluntarily reduce their off-peak demand receive financial incentives in the form of electricity bill reductions, provided by the RCMG operator, to encourage participation and support system resilience. This approach promotes consumer convenience and system reliability, as described below:

- **Consumer Convenience**: The impact of power outages on households varies by time of day,

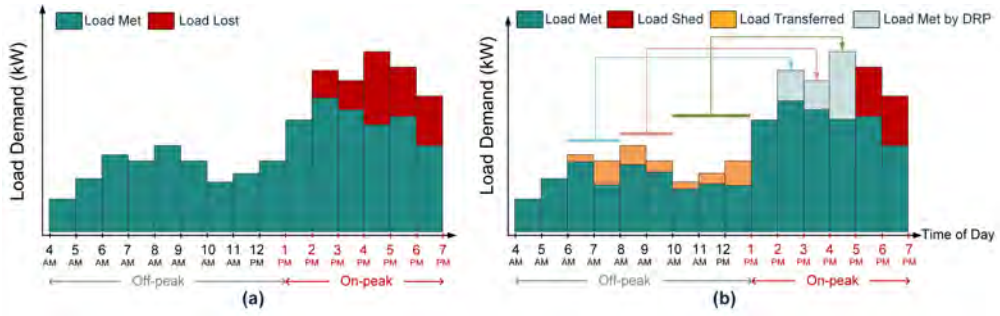

Figure 2: The proposed DRP. The figure shows how DRP changes the allocation of RCMG power during hours of outage. Hours highlighted in red represents on-peak hours for which load-curtailing is prohibited.

with peak hours like mornings and nights in winter or midday in summer being particularly challenging due to extreme temperatures. Storing power for peak hours ensures households have the necessary supply to maintain comfort and resilience during such critical times.

- **System Reliability**: During power outages, RCMG components face increased stress, especially during peak hours, potentially causing malfunctions or reduced efficiency. The proposed DRP enhances system reliability by: i) balancing the load and preventing overload, ii) extending component longevity by reducing operation at maximum capacity, iii) improving efficiency by staying within device limits, and iv) minimizing the risk of failure due to overheating during peak hours.

3.1 RCMG Formulation

We propose a two-stage mixed-integer stochastic programming model for planning and operation of the RCMG. In the first stage, the model determines the optimal location and capacity of devices to minimize initial investment costs, while adhering to constraints related to candidate locations, budget, and capacity limits. The second stage focuses on expansion costs and operation of the devices, incorporating uncertainties including hourly load demand, outage duration, and annual load demand growth. The key assumptions underlying the RCMG model are outlined as follows.

- Two investment decisions are made: one in the first year and another in the year n, with two representative years considered, each comprising of 12 months. Scheduling decisions are based on a representative week for each month, with costs scaled to a yearly basis using an

adjustment parameter to account for non-integer week alignments.

- Linear battery degradation is assumed for simplicity, with degradation modeled throughout n years of operation, including calendar and cyclic aging. In addition, inversion and conversion rates, as well as ES charging and discharging rates, are assumed to be fixed.

- Equity is addressed through investment and scheduling by assigning renewable energy subsidies and load shedding penalties, quantified using a power outage-risk integrated social vulnerability index (PO-RSVI) and WTP for emergency power supply parameters, which will be discussed in Section 5.

3.1.1 Stage 1: First Year Investment

We denote the life-time of RCMG by N. Let's consider F_l, $C_d, O_d = \gamma^{opr} C_d$ as the fixed cost of selecting location $l \in L$, the unit cost, and the operation cost of device $d \in \mathcal{D} = \{es, pv, dg\}$, respectively. The parameter $\gamma^{opr} \in [0, 1]$ is to set the operational cost as a percentage of unit cost. Let $u_l^I \in \mathbb{B}$ and $x_{l,d}^I \in \mathbb{Z}_+$ determine selection of location l and capacity of device d to be installed, respectively. Given the subsidy rate β available for land procurement and device unit price, along with the community's SV level V, the total cost is determined as shown in (1) subject to the budget constraint (2) and device capacity limits (3). The parameter V is used to determine the equitable allocation of subsidies, ensuring that more vulnerable communities receive a higher subsidy rate, approaching the nominal rate β.

$$C^I = \sum_{l \in \mathcal{L}} \sum_{d \in \mathcal{D}} [(1 - \beta V)\big(F_l \cdot u_l^I + C_d \cdot x_{l,d}^I\big) + O_d \cdot x_{l,d}^I] \tag{1}$$

$$\sum_{l \in \mathcal{L}} \sum_{d \in \mathcal{D}} (1 - \beta V)(F_l \cdot u_l^I + C_d \cdot x_{l,d}^I) \leq B^I \tag{2}$$

$$\underline{x}_{l,d}^I \cdot u_l^I \leq x_{l,d}^I \leq \overline{x}_{l,d}^I \cdot u_l^I, \qquad \forall l \in \mathcal{L}, d \in \mathcal{D} \tag{3}$$

3.1.2 Stage 2: Expansion and Scheduling

Let $x_{l,d,s}^E \in \mathbb{Z}_+$ be the increase in the capacity of device $d \in \mathcal{D}$ at location $l \in L$ under scenario $s \in \mathcal{S}$. We denote the power scheduling decisions by $y_{t,g,s} \in \mathbb{R}_+$, where the super-index refers to the usage type of power and the sub-indices refer to the hour of week $t \in \mathcal{T}$, in representative year

$g \in \mathcal{G} = \{\mathcal{G}_I, \mathcal{G}_E\}$, and under scenario $s \in \mathcal{S}$.

Concerning costs, the expansion cost (C_s^E) is defined in (4). The cost of load shedding (C_s^{LS}) is calculated in (5) with $y_{t,g,s}^{ls}$ and r_t^{ls} representing the amount of load shedding and the corresponding penalty, respectively. Cost of curtailing power (C_s^C) in PV and DG is calculated in (6), with $y_{t,g,s}^{,c}$ and r^c referring to the amount of curtailment and the penalty, respectively. The cost of import from/export to the grid (C_s^{IE}) is calculated in (7). The cost of fuel burnt by DG (C_s^F) is calculated in (8) with $y_{t,g,s}^{dg,\cdot}$ and f representing DG power and fuel cost, respectively. RCMG main revenue (C_s^R) is calculated in (9) using parameter e^l as the associated RCMG electricity price. Lastly, the incentives for load reduction by consumers (C_s^{IN}) are calculated in equation (10), where $y_{t,g,s}^{drp}$ represents the amount of load reduction, and e^{drp} denotes the incentive allocated.

$$C_s^E = \sum_{l\in\mathcal{L}} \sum_{d\in\mathcal{D}} (1-\beta V) C_d x_{l,d,s}^E + x_{l,d,s}^E O_d, \qquad \forall s \in \mathcal{S} \tag{4}$$

$$C_s^{LS} = \sum_{g\in\mathcal{G}} \sum_{t\in\mathcal{T}} r_t^{ls} \cdot y_{t,g,s}^{ls}, \qquad \forall s \in \mathcal{S} \tag{5}$$

$$C_s^C = \sum_{g\in\mathcal{G}} \sum_{t\in\mathcal{T}} r^c (y_{t,g,s}^{pv,c} + y_{t,g,s}^{dg,c}), \qquad \forall s \in \mathcal{S} \tag{6}$$

$$C_s^{IE} = \sum_{g\in\mathcal{G}} \sum_{t\in\mathcal{T}} e^{im} \cdot y_{t,g,s}^{im} - e^{ex} \cdot y_{t,g,s}^{ex}, \qquad \forall s \in \mathcal{S} \tag{7}$$

$$C_s^F = \sum_{g\in\mathcal{G}} \sum_{t\in\mathcal{T}} f (y_{t,g,s}^{dg,es} + y_{t,g,s}^{dg,l} + y_{t,g,s}^{dg,c}), \qquad \forall s \in \mathcal{S} \tag{8}$$

$$C_s^R = \sum_{g\in\mathcal{G}} \sum_{t\in\mathcal{T}} \gamma^l e^{im} (y_{t,g,s}^{es,l} + y_{t,g,s}^{pv,l} + y_{t,g,s}^{dg,l}), \qquad \forall s \in \mathcal{S} \tag{9}$$

$$C_s^{IN} = \sum_{g\in\mathcal{G}} \sum_{t\in\mathcal{T}} e^{drp} \cdot y_{t,g,s}^{drp}, \qquad \forall s \in \mathcal{S} \tag{10}$$

Considering all, the expected cost of expansion and scheduling stage ($\mathbb{E}_s[Q_s]$) is calculated in (12), following the scenario costs Q_s in (11), where ξ generalizes the representative weeks to the full year, and p_s denotes the probability of scenario s.

$$Q_s = C_s^E + \xi (C_s^{LS} + C_s^C + C_s^{IE} + C_s^F - C_s^R - C_s^{IN}) \tag{11}$$

$$\mathbb{E}_s[Q_s] = \sum_{s\in\mathcal{S}} p_s \cdot Q_s \tag{12}$$

Expansion Constraints: Constraints (13) and (14) address budget and location limitations in the second stage. The former enforces expansion budget (B^E) adherence, while the latter ensures that added device capacities are assigned only to locations selected in the first stage, without exceeding capacity limits.

$$\sum_{l\in\mathcal{L}}\sum_{d\in\mathcal{D}}(1-\beta V)C_d x^E_{l,d,s} \le B^E \tag{13}$$

$$\underline{x}^E_{l,d}\cdot u^I_l \le x^E_{l,d,s} \le \overline{x}^E_{l,d}\cdot u^I_l, \quad \forall l\in\mathcal{L}, d\in\mathcal{D} \tag{14}$$

Scheduling Constraints: To model scheduling, we determine the available capacity of devices, denoted by $A^{\cdot}_g$, after considering expansion and degradation. We schedule devices for a representative year both before and after expansion, using the sets of months $\mathcal{G}_I$ and $\mathcal{G}_E$, respectively. We estimate that ES energy capacity degrades every year at rate d^{es}. In the year following the expansion, the first-installed ES devices are expected to be degraded by $(1-d^{es})^n\%$ (15). With negligible PV and DG degradation, post-expansion capacity is the sum of initial-year and newly added capacities, as shown in (16) and (17), respectively.

$$A^{es}_g = \begin{cases} \sum_{l\in\mathcal{L}} x^I_{l,es} & \text{if } g\in\mathcal{G}_I \\ \sum_{l\in\mathcal{L}}(1-d^{es})^n x^I_{l,es} + x^E_{l,es,s} & \text{if } g\in\mathcal{G}_E \end{cases} \tag{15}$$

$$A^{pv}_g = \begin{cases} \sum_{l\in\mathcal{L}} x^I_{l,pv} & \text{if } g\in\mathcal{G}_I \\ \sum_{l\in\mathcal{L}} x^I_{l,pv} + x^E_{l,pv,s} & \text{if } g\in\mathcal{G}_E \end{cases} \tag{16}$$

$$A^{dg}_g = \begin{cases} \sum_{l\in\mathcal{L}} x^I_{l,dg} & \text{if } g\in\mathcal{G}_I \\ \sum_{l\in\mathcal{L}} x^I_{l,dg} + x^E_{l,dg,s} & \text{if } g\in\mathcal{G}_E \end{cases} \tag{17}$$

To implement DRP, we use variables ($y^{drp}_{t,g,s}$) that determines the amount of load curtailed at time $t\in\mathcal{T}$. The load balance constraint (18) is then introduced with variables $y^{es,l}_{t,g,s}, y^{dg,l}_{t,g,s}, y^{pv,l}_{t,g,s}, y^{g,l}_{t,g,s}$ denoting the amount of power directed from ES, PV, DG, and grid to serve the load ($L_{t,g,s}$) and $y^{ls}_{t,g,s}$ denoting load shedding. We allow partial load curtailment without significant load shedding,

which is implemented in (19) using γ^{drp} as the DRP rate.

$$y^{es,l}_{t,g,s} + y^{dg,l}_{t,g,s} + y^{pv,l}_{t,g,s} + y^{g,l}_{t,g,s} + y^{ls}_{t,g,s} + y^{drp}_{t,g,s} = L_{t,g,s}, \qquad \forall t \in \mathcal{T}, g \in \mathcal{G}, s \in \mathcal{S} \tag{18}$$

$$\sum_{t'=t+1}^{T} y^{drp}_{t,t',g,s} \leq \gamma^{drp} \cdot L_{t,g,s}, \qquad \forall t \in \mathcal{T}, g \in \mathcal{G}, s \in \mathcal{S} \tag{19}$$

Constraints (20) and (21) limit the usage of power generated by PV and DG devices, which can either serve the load ($y^{\cdot,l}_{t,g,s}$), be sold to the grid ($y^{\cdot,g}_{t,g,s}$), or stored in ES devices ($y^{\cdot,es}_{t,g,s}$). Parameters λ define the efficiency of PV and DG devices, with PV efficiency depending on time and scenario.

$$y^{pv,l}_{t,g,s} + y^{pv,g}_{t,g,s} + y^{pv,es}_{t,g,s} \leq \lambda^{pv}_{t,s} \cdot A^{pv}_{g}, \quad \forall t \in \mathcal{T}, g \in \mathcal{G}, s \in \mathcal{S} \tag{20}$$

$$y^{dg,l}_{t,g,s} + y^{dg,g}_{t,g,s} + y^{dg,es}_{t,g,s} \leq \lambda^{dg} \cdot A^{dg}_{g}, \quad \forall t \in \mathcal{T}, g \in \mathcal{G}, s \in \mathcal{S} \tag{21}$$

The power exported to the grid ($y^{ex}_{t,g,s}$) is supplied only by PV. The imported power from the grid ($y^{im}_{t,g,s}$) can either be stored in ES or directly used to meet the demand. These relationships are formulated in (22) and (23), respectively.

$$y^{ex}_{t,g,s} = y^{pv,g}_{t,g,s}, \qquad \forall t \in \mathcal{T}, s \in \mathcal{S}, g \in \mathcal{G} \tag{22}$$

$$y^{im}_{t,g,s} = y^{g,es}_{t,g,s} + y^{g,l}_{t,g,s}, \qquad \forall t \in \mathcal{T}, s \in \mathcal{S}, g \in \mathcal{G} \tag{23}$$

To ensure an islanded mode during an outage, the constraint (24) is defined. Denoting $\mathcal{I}_s$ as the set of hours for which there is an outage in scenario s, for any $t \in \mathcal{I}_s$ grid transactions are prohibited.

$$y^{ex}_{t,g,s} + y^{im}_{t,g,s} = 0, \quad \forall t \in \mathcal{I}_s, g \in \mathcal{G}, s \in \mathcal{S} \tag{24}$$

Lastly, we ensure the flow of power in ES devices is feasible. Defining ES energy level as $E_{t,g,s}$, equation (25) ensures that ES devices start the scheduling horizon at their maximum allowable energy ($\overline{SOC}$). For other time periods, the energy level is affected by charging, discharging, and load curtailing as described in (26). In this constraint, λ^{es} is ES efficiency parameter in charging and discharging and η^{i}, η^{c} are the inversion and conversion rates, respectively. The constraint

(27) ensures that energy level at ES is always within the manufacturer recommended limits, which includes $\underline{SOC}$ as the minimum state of charge.

$$E_{1,g,s} = \overline{SOC} \cdot A_g^{es}, \quad \forall g \in \mathcal{G}, s \in \mathcal{S} \tag{25}$$

$$E_{t+1,g,s} = E_{t,g,s} + \lambda^{es}(y_{t,g,s}^{pv,es} + y_{t,g,s}^{dg,es} + \eta^c \cdot y_{t,g,s}^{g,es}) - \frac{\eta^i}{\lambda^{es}}(y_{t,g,s}^{es,l} + y_{t,g,s}^{es,g}), \quad \forall t \in \mathcal{T}, g \in \mathcal{G}, s \in \mathcal{S} \tag{26}$$

$$\underline{SOC} \cdot A_g^{es} \leq E_{t,g,s} \leq \overline{SOC} \cdot A_g^{es}, \quad \forall g \in \mathcal{G}, s \in \mathcal{S} \tag{27}$$

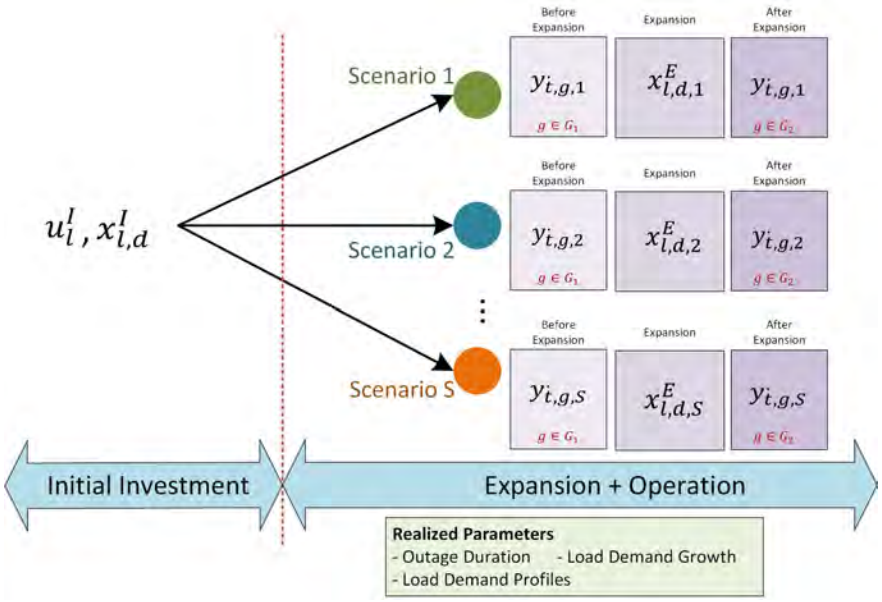

Figure 3: The diagram of the proposed two-stage stochastic model for RCMG.

Figure (3) presents the diagram of the proposed two-stage stochastic model with the decisions made at each stage. The RCMG investment and operational cost minimization problem then is as follows:

$$\mathbf{P}: \min \quad C^I + \mathbb{E}_s[Q_s] \tag{28}$$

$$\text{s.t.} \quad (1) - (27)$$

3.1.3 Solution Methodology

Problem **P** in (28) involves a large number of independent scenarios coupled through first-stage decisions, which makes solving the problem with conventional MIP methods, such as Branch-and-Bound, computationally challenging due to its scale. However, its structure is well-suited for decomposition into smaller scenario-based subproblems using Benders Decomposition. In this approach, the first-stage problem is significantly reduced in size and referred to as the master problem (MP), while each scenario is addressed through a corresponding separation problem (SP). To accommodate the integer requirements—particularly in the MP, a Branch-and-Bound framework is applied, resulting in a Benders Branch-and-Cut algorithm.

The algorithm was first proposed in [51], and further studied in the literature. The MP involves minimizing C^I in addition to an estimation of the second stage costs, η, while only considering first stage constraints. The SP is then minimizing the costs of each scenario $s \in \mathcal{S}$, Q_s, while considering only the constraints associated with that scenario. Let x and y denote all variables in the first and second stage, respectively. The abstract form of MP and SP is then as follows:

$$
\begin{aligned}
\text{MP}: \min \quad & c^\top x + \eta \\
s.t. \quad & Ax \geq b \\
& \eta \geq -M \\
& x \in \mathbb{Z}_+, \eta \in \mathbb{R} \\
\text{SP}: \min \quad & q_s^\top y_s \\
s.t. \quad & W y_s \geq r_s - T_s x^* \\
& y_s \in \mathbb{R}_+
\end{aligned}
$$

The approach involves solving problem MP through the Branch & Bound tree. Each time an integer solution is found, SP for each scenario is solved, generating an optimality cut as represented in (29), which is then added to the corresponding node of the tree. Regarding terminology in the optimality cut, p_s represents the probability of scenario, π_s is the dual multiplier of constraints, T_s denotes the coefficient matrix of coupling decisions variables, and r_s denotes the right hand side of constraints in the subproblem of scenario s. The node is subsequently re-optimized and the

previous integer solution is removed if duality gap in all SP problems is not closed. This process continues until optimality conditions of SP are met.

In the proposed model, the integrality constraints of $x^E_{l,d}$ are relaxed to facilitate the use of Benders Decomposition. This assumption is valid because the cost of the fractional part of the decision variable is negligible compared to the total investment costs, due to the relatively low unit cost of devices. Additionally, as the sub-problems are always feasible for any first-stage solution, we utilize only optimality cuts. The pseudo-code for the Benders Branch & Cut method is provided in Algorithm 1.

$$\eta \geq \xi - \zeta^\top x \tag{29}$$

$$\zeta = \sum_{s\in\mathcal{S}} p_s \pi_s^\top T_s, \quad \xi = \sum_{s\in\mathcal{S}} p_s \pi_s^\top r_s \tag{30}$$

Algorithm 1 Benders Branch & Cut algorithm

Initialize: Iteration $k \leftarrow 0$, $\eta \leftarrow -\infty$, active nodes $T^k \leftarrow \{0\}$, tolerance $\epsilon > 0$, upper bound UB $\leftarrow \infty$, lower bound LB $\leftarrow -\infty$.
Solve MP for root node $t = 0$, obtain v^0.
while $|\text{UB} - \text{LB}| > \epsilon$ **do**
  while True **do**
    Update lower bound: LB $\leftarrow \min_{t\in T^k}\{v^t\}$; let $\bar{t}$ be the corresponding node.
    if $x^{\bar{t}} \in \mathbb{Z}$ **then**
      $t(k) \leftarrow \bar{t}$
      break
    end if
    Branch on $x^{\bar{t}}$; add children, remove $\bar{t}$ from T^k.
    Solve MP for $\bar{t}_1$, $\bar{t}_2$, obtain $v^{\bar{t}_1}, v^{\bar{t}_2}$; discard infeasible nodes.
  end while
  for $s \in S$ **do**
    Solve SP using $x^{t(k)}$ to get duals π_s.
  end for
  Compute $\eta^k = \xi - \zeta^\top x^{t(k)}$ using (30).
  Derive cut (29); add to MP at node $t(k)$.
  Resolve MP at $t(k)$ to get new $x^{t(k)}$.
  if Optimality cut is not violated **then**
    Update UB $\leftarrow \min(\text{UB}, v^{t(k)})$.
    Prune $t(k)$ from T^k.
  end if
  $k \leftarrow k + 1$
end while

4 Energy Resilience Metrics

Resilience, as a multi-discipline concept, refers to a system's ability to return to its original functionality after exposure to an adversity [52]. Regardless of the application, resilience is suggested to have the following properties [52]: i) Robustness: the ability of elements and units to endure stress or demand without degradation or function loss, ii) Redundancy: the availability of substitutes that can meet functional requirements during disruptions, iii) Rapidity: the ability to meet priorities and achieve goals promptly to contain losses and prevent future disruptions, and iv) Resourcefulness: the ability to identify problems, prioritize, and mobilize resources during disruption.

To quantify resilience in our RCMG, three metrics Φ, Λ, and E are selected based on the literature on power systems resilience metrics [53]. The metric Φ capture the rate at which resilience declines. The metric Λ defines how low resilience drops, and the metric E captures how long the degraded state lasts after the disaster, until the system regains its pre-event strength. Quantifying resilience metrics require calculation of relevant indicators. Here, building upon the concept of each resilience metric and inspiring from literature, we define three resilience indicators to quantify Φ, Λ and E, respectively (see Table (1)).

To quantify Φ, we measure the duration (in hours) that the microgrid continues serving at least 50% of its load after the onset of an outage. The ratio of this duration to the total outage time defines Φ, an indicator of the system's *robustness*, reflecting its ability to resist failure under stress. A higher value indicates greater robustness, as shown below:

$$\Phi = \sum_{g \in \mathcal{G}} \sum_{s \in \mathcal{S}} p_s \cdot \left(\frac{\min\{t \in \{0, \ldots, \mathcal{T}-1\} : y^{ls}_{t,g,s} < 0.5 L_{t,g,s}\}}{\mathcal{I}_s}\right).$$

For Λ, we define it as the ratio of the total load demand served during the outage to the total load demand over the same period. Widely used in the literature [4, 54], this indicator reflects the system's *resourcefulness*, or its effectiveness in utilizing available assets to meet demand post-disruption. It also captures the lowest level to which resilience drops, where a lower value indicates significant load loss, and a higher value reflects more effective resource management under adverse

conditions. The metric Λ is calculated as follows

$$\Lambda = \sum_{g\in\mathcal{G}}\sum_{t\in\mathcal{T}}\sum_{s\in\mathcal{S}} p_s \cdot \left(\frac{L_{t,g,s} - y^{ls}_{t,g,s}}{L_{t,g,s}}\right).$$

To quantify E, we consider the total number of hours during which the load is at least partially served, for instance less than 50% is lost. The ratio of this duration to the total outage duration defines E, following a similar approach in [5]. This indicator reflects system *redundancy* by capturing its ability to maintain service through alternative or backup options. Higher values, indicating fewer hours of unmet load, correspond to stronger redundancy in supporting critical loads during partial system operation. The metric E is calculated as follows

$$\mathrm{E} = \sum_{g\in\mathcal{G}}\sum_{s\in\mathcal{S}} p_s \left(\frac{\sum_{t\in\mathcal{T}} \mathbf{1}\{y^{ls}_{t,g,s} < 0.5 L_{t,g,s}\}}{\mathcal{I}_s}\right),$$

where $\mathbf{1}\{.\}$ is the indicator function (1 if the condition is true, 0 otherwise).

The proposed model is designed to enhance the resilience metrics above. To improve Φ, the load-shedding penalty is higher in the early hours of an outage and gradually decreases, promoting prolonged service. To improve Λ, penalties are scaled by community WTP, with more vulnerable communities—who tend to have lower WTP [21]—assigned higher penalties, prioritizing their load delivery and reinforcing both Λ and E.

Table 1: Proposed community energy resilience metrics and their properties.

Metric	Property	Indicator
Φ	Robustness	The proportion of outage duration during which the microgrid sustains at least 50% of load demand.
Λ	Resourcefulness	The proportion of total load demand satisfied during the outage period.
E	Redundancy	The Proportion of outage duration during which load demand is at least 50% satisfied.

5 Case Studies

5.1 Community Specifications

Three residential communities in Texas are selected which include: 1) Dove Springs in Austin, 2) Sunnyside in Houston, and 3) Rogers Washington in Austin. Their key characteristics are summarized in Table (2). Data on PO-RSVI and WTP are derived from our recent study of outage impacts on vulnerable communities [21]. PO-RSVI captures susceptibility to harm from outages across infrastructural, socio-economic, health, and accessibility dimensions. Social vulnerability metrics like this are increasingly used to link inequality to disaster impacts and guide equitable policies [55]. WTP informs demand-side pricing by indicating how much consumers are willing to pay for reliability, clean energy, or uninterrupted service, helping utilities design fair and cost-reflective pricing schemes [56]. Here, PO-RSVI and WTP inform equity in the subsidy rates, the load shedding costs, and the pricing for RCMG emergency power supply.

Grid electricity prices are obtained from market data, and installation spaces were based on church and school roof areas in the communities. Winter peak hours are considered at 6–10 AM and 6–10 PM during January, February, and March, while summer peak hours are 1–7 PM in June, July, August, and September. Load curtailing is prohibited during these periods.

Table 2: Characteristics for the community case studies.

Characteristics	Community 1	Community 2	Community 3
Power Outage-Risk integrated Social Vulnerability Index (PO-RSVI)	1.00	0.59	0.00
Willingness-To-Pay (WTP)	0.2764	0.2567	0.5157
Count of Households	40	20	20
Average Land Price ($/sq/yr)	20.40	11.80	22.80
Average Electricity Price ($/kW)	0.14	0.15	0.14
Grid Buyback Price ($/kW)	0.097	0.120	0.097
Available Space for PV (sq^2)	265,785	69,442	87,846
Available Budget (B^I, B^E)	$1M, $0.1M	$1M, $0.1M	$1M, $0.1M

To quantify load shedding penalty (r^{ls}) we use WTP as shown in Equation (31). Vulnerable households generally have lower WTP due to limited capacity to compensate for outage costs [21]. To capture this, the penalty scales inversely with WTP using the factor $(2 - \text{WTP})$, which ranges from 1 to 2. This factor is multiplied by the grid power price (e^{im}) and a scaling parameter α, reflecting the investor's priority to reduce load shedding. In our analysis, we set $\alpha = 5$. Additionally,

to model incentives for DRP and load curtailment, we use the grid import price and the DRP rate γ^{drp} as shown in (32). Specifically, for each kW of reduced consumption, the consumers receive a bill discount, proportional to γ^{drp}. Since load curtailment is a substantial burden, the incentive must be sufficiently high to encourage participation. Social vulnerability V = PO-RSVI is used to determine the equitable allocation of subsidies, with a maximum rate β (see (33)).

$$r^{ls} = \alpha(2 - \text{WTP})e^{im} \tag{31}$$

$$e^{drp} = (1 + \gamma^{drp})e^{im} \tag{32}$$

$$\text{subsidy allocated} = (1 - \beta V) \tag{33}$$

5.2 RCMG Specification

Table (3) provides the economic, technical, and operational parameters used in RCMG, detailing device costs, efficiency rates, pricing factors, and planning horizons. Note that PV degradation is not considered, as it is typically negligible; around 0.3–0.8% per year.

Table 3: Specification of devices and parameters in the proposed RCMG model.

Parameter	Description	Value
C_{es}, C_{pv}, C_{dg}	ES, PV, DG device unit price	380, 1200, 500 \$/kW
$\overline{SOC}$, $\underline{SOC}$	ES limits on state of charge	0.9, 0.1
γ^{opr}	Device operation cost factor	5%
γ^{drp}	DRP rate	0.2%
γ^{l}	RCMG electricity price rate	0.9
λ^{dg}, λ^{es}	DG efficiency, ES charge efficiency	40%, 90%
f	DG fuel consumption efficiency (fuel cost× fuel usage)	3.12 × 0.07
d^{es}, d^{dg}	Annual degradation	2.0%
e^{im}	Grid import price (Community 1, 2, 3)	(0.14, 0.15, 0.14) \$/kW
e^{ex}	Grid export price (Community 1, 2, 3)	(0.097, 0.12, 0.097) \$/kW
r^{c}	PV curtailment penalty (Community 1, 2, 3)	(0.14, 0.15, 0.14) \$/kW
η^{i}, η^{c}	ES inversion and conversion	90%
N, n	Planning horizon, Expansion year	20, 10

5.3 Uncertain Parameters and Scenario Generation

This study considers three uncertain parameters: daily load demand, annual load growth, and power outage duration. Hourly load demand data for Texas residential buildings were retrieved from the End-Use Load Profiles for the U.S. Building Stock [57]. Load uncertainties across communities are

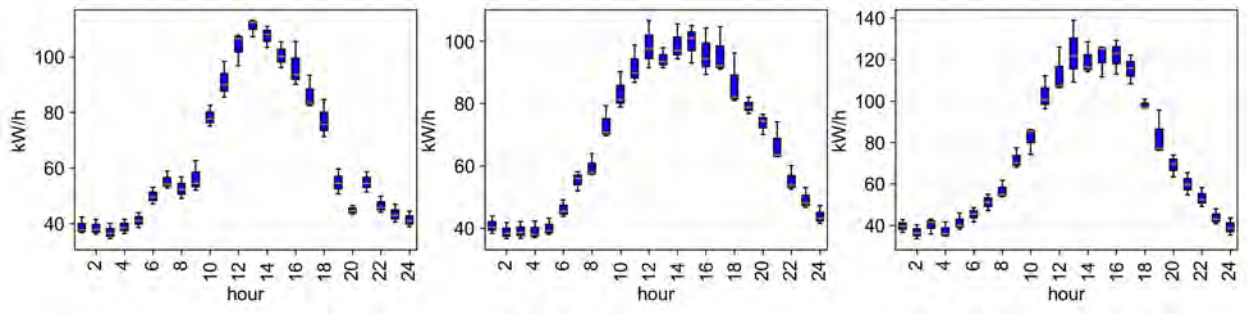

Figure 4: Box-plots showing the distribution of load demand across the communities.

presented in Figure (4). For power outage duration, we utilized records of weather-related electricity disruptions in Texas from 2002 to 2023, sourced from the Office of Cybersecurity, Energy Security, and Emergency Response (CESER) [1]. Annual load growth utilizes Residential Sector Energy Consumption Estimates data for Texas from 1960 to 2021 [58]. The probability distributions for both outage duration and annual demand growth are shown in Figure (5). Regarding power generated by PV, hourly solar energy generation data over one year for each PV unit is retrieved from the PVWatts Calculator (NREL) tool.

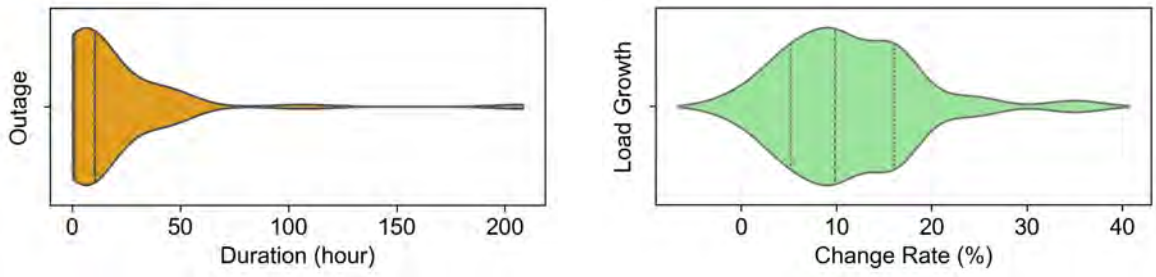

(a) Power Outage Duration

(b) Load Growth Rate

Figure 5: Violin-plots showing the (a) distribution of outage duration in hours and (b) load demand growth rate (%).

The uncertainties are represented by multiple scenarios for the corresponding parameters, generated using two methods: (i) Roulette Selection and (ii) Generative Adversarial Networks (GAN). (i) In Roulette Selection, the probability density function (PDF) of the uncertain variable is divided into discrete blocks, and a block is selected based on a randomly generated number. This method generates scenarios for power outage duration and annual load demand growth. (ii) GAN uses two neural networks: the Generator (G), which creates fake samples, and the Discriminator (D), which distinguishes real from fake samples. G aims to fool D, leading to Nash equilibrium when

generated samples are indistinguishable from real ones. Here, Roulette Selection is used for outage duration and load demand growth and GAN is used to generate scenarios for weekly load demand. Supplementary Figure 1 illustrates the scenario generation methods.

5.4 Implementation Details

As this study is application-driven, formal validation against simplified benchmarks is not included, consistent with similar literature. The implementation considered 27 generated scenarios. The model is solved in Python 3.10, using Gurobi Optimizer 10.0.3 on a Windows system with an Intel(R) 5220 CPU @ 2.20 GHz. The solution process explored approximately 400 nodes within 540 seconds, generating 219 lazy constraints and achieving convergence with a final MIP gap of 0.27%, indicating a high-quality near-optimal solution. The global gap reported by Gurobi inherently accounts for the relaxed second-stage integrality, confirming that any sub-optimality remains negligible for the intended application.

6 Findings and Insights

This section presents an analysis of i) RCMG costs and resilience under four strategic scenarios combining expansion and DRP participation, ii) the RCMG economic benefits, iii) the RCMG performance under prolonged outages, iv) sensitivity analysis of key parameters, and v) the scalability of the RCMG design.

6.1 Performance of Resilience Strategies

The performance of the RCMG is examined under the following four strategies to understand the individual and combined effects of system expansion and DRP:

- **Strategy 1 (S1)-No DRP, No Expansion**: Serves as the baseline case and reflects current infrastructure and demand without DRP flexibility mechanisms.
- **Strategy 2 (S2)-Expansion Only (No DRP)**: Involves investment in additional PV and/or ES after 10 years but no DRP is implemented.

- **Strategy 3 (S3)-DRP Only (No Expansion)**: Implements demand-side load curtailing without expansion after 10 years. It explores how flexible demand can alleviate system stress.
- **Strategy 4 (S4)-DRP + Expansion**: Combines both supply- and demand-side strategies and represents a coordinated investment in infrastructure and operational flexibility.

For DRP implementation, a rate of 20% is considered. These scenarios provide a structured basis for evaluating trade-offs between infrastructure investments and operational strategies in supporting microgrid performance.

Table 4: The RCMG performance under four strategies in each community.

Community		Investment ($)	Expansion ($)	ES (kW)	PV (kW)	DG (kW)	Bill Savings ($)	Incentives ($)
1	S1	134,244	0	(83, 0)	(166, 0)	(25, 0)	3.08%	0
	S2	112,992	66,161	(69, 32)	(138, 89)	(25, 6)	3.46%	0
	S3	129,056	0	(80, 0)	(159, 0)	(25, 0)	12.70%	333
	S4	111,725	62,733	(69, 30)	(136, 84)	(25, 6)	13.20%	322
2	S1	166,119	0	(88, 0)	(176, 0)	(21, 0)	3.11%	0
	S2	112,280	61,303	(58, 25)	(116, 70)	(21, 6)	2.85%	0
	S3	159,985	0	(85, 0)	(169, 0)	(21, 0)	12.69%	342
	S4	112,280	60,927	(58, 24)	(116, 69)	(21, 5)	12.46%	340
3	S1	132,608	0	(30, 0)	(120, 0)	(25, 0)	2.36%	0
	S2	128,319	79,559	(30, 26)	(120, 69)	(16, 15)	3.41%	0
	S3	128,586	0	(29, 0)	(116, 0)	(25, 0)	12.23%	348
	S4	128,318	66,608	(30, 21)	(120, 56)	(16, 15)	13.00%	349

Strategy Analysis

Table (4) presents the optimal solutions for each strategy regarding the amount of investment and expansion, capacity of devices, households monetary benefits in all communities. Note that for capacity of devices, the number on the left in the parenthesis is first year investment and the number on the right is the expansion capacity in year 10.

For Community 1 (PO-RSVI = 1.00), comparing Strategy 2 (only expansion) with Strategy 1 (no expansion, no DRP), there is an 15.86% reduction in the first-year investments, with expected expansion of 66,161$. If demand grows significantly over time, expansion requirements increase; conversely, if demand remains low, required expansion could be smaller. Strategy 2 also yields a 3.46% bill savings, which is 12.3% higher than that for Strategy 1. In Strategy 3 (expansion only), a 3.87% reduction in investment is observed, benefiting investors. Additionally, DRP offers

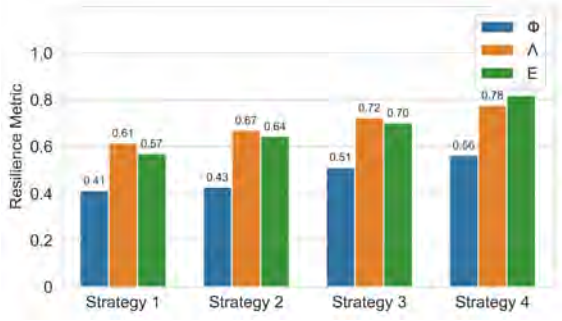

(a) Community 1

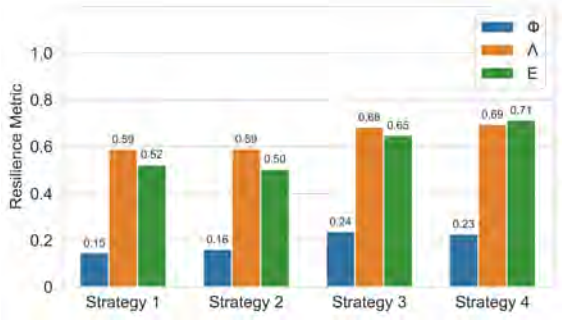

(b) Community 2

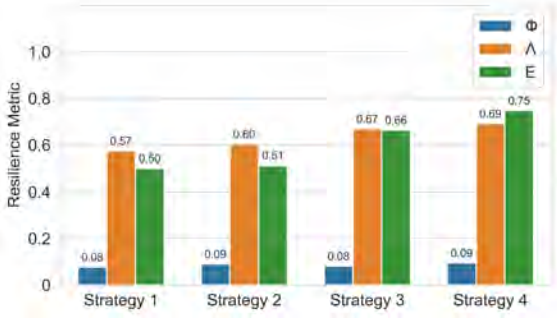

(c) Community 3

Figure 6: Energy resilience metrics for the four strategies in each community.

substantial bill savings of 12.7%, with expected incentives of $333. Strategy 4 achieves the highest investment reduction of 16.77%, requiring only $62,733 for expansion—approximately 5% less than Scenario 2. Its bill savings are slightly higher than Strategy 3, and its incentives are comparable, but the additional investment reduction makes Strategy 4 the most cost-effective strategy.

For Community 2 (PO-RSVI = 0.59), similar to Community 1, with Strategy 2 (expansion only), a 32.42% reduction in first-year investment is observed, compared to the baseline, though bill savings show no improvement. Strategy 3 (DRP only) results in 3.69% reduction in investment and 12.69% bill savings—significantly higher than the baseline. Additionally, DRP provides annual household incentives averaging $342, effectively encouraging consumer participation and contributing to demand-side flexibility. Lastly, Strategy 4 provides the same solution to Strategy 2 in investment, bill savings, and incentives, however expansion costs are reduced by 0.6%, making it more cost-effective strategy.

Community 3 (PO-RSVI = 0.00), exhibits the same patterns to Communities 1 and 2 in terms of monetary benefits. As shown in Table (4), Strategy 2 (expansion only) reduces investments up to 3.23% with a slight improvement in electricity bills, from 2.36% to 3.41%. Strategy 3 (DRP

only) reduces investments by 3.30% and yields a 12.23% reduction in electricity bills and $348 in annual bill incentives. When Strategy 4 is applied, investment decreases the most and electricity bills improve to 13%, and $349 incentives are provided to the community households.

Regarding resilience, Figures in (6) present changes in the resilience metrics over the four strategies for each community. In Community 1 (Figure (6a), strategy 2 improves Φ up to 0.43 through added capacity, significantly strengthening robustness of the community to the shock of outages. Improvements are also observable in Λ and E up to 0.67 and 0.64, respectively. Strategy 3 increases all the metrics Φ, Λ, and E by 24%, 18%, and 22%, respectively. Although DRP enables load curtailment, which could potentially reduce Φ, the observed improvement underscores the framework's effectiveness in not only preserving but also boosting it significantly. Strategy 4, with both DRP and expansion improves all metrics—up to 0.56 for Φ and 0.78 for Λ and 0.82 for E, demonstrating its strength of the combined approach. That is to say, both expansion and DRP provide resilience benefits, and their combination yields the greatest overall gains.

For Community 2 (Figure (6b), the Φ metric is noticeably lower than that of Community 1 in all strategies. This highlights the framework's effectiveness in boosting robustness for highly vulnerable consumers. Strategy 2 does not show noticeable changes in resilience when expansion is applied. Despite the reduction in investment, resilience is preserved. Strategy 3, on the other hand, exhibits the same pattern observed in Community 1. This strategy improves the metrics Φ, Λ, and E by 60%, 15%, and 25%, respectively. Once again, the larger improvement in Φ reinforces the claim that DRP enhances the community's robustness to outage shocks, besides its effectiveness in boosting resourcefulness and redundancy. Similar improvements are observed in Strategy 4, making it the most effective option when its monetary benefits are also considered.

In Community 3 (Figure (6c), similar patterns are observed. Strategy 2 contributes to improvements in two resilience metrics, Λ and E, with no significant enhancement in Φ. Strategy 3 also primarily improves Λ and E. The combined Strategy 4 follows the same pattern, showing only a slight improvement in Φ. These observations suggest that in less vulnerable areas, both expansion and DRP tend to enhance the resourcefulness and redundancy of emergency power supply, rather than mitigating the shock of outages. This is reasonable, as Community 2 households are better prepared for outages. Therefore, prioritizing continuity of power service is recommended to achieve monetary benefits while maintaining resilience.

6.2 Cost-Effectiveness of DRP

While some operational/monetary benefits of the DRP are evident above, a detailed comparison against the PV deployment alternative requires assessing total system investment. To accurately evaluate this trade-off, we compare the Levelized Annual Cost of DRP capacity to the cost of equivalent PV capacity. This analysis incorporates a conservative proxy implementation cost for DRP, set at $\$200/kW$ of realized load reduction capacity, consistent with costs cited in technical literature [59]. Furthermore, the PV deployment cost is adjusted to include the annualized cost of land acquisition.

As shown in Table (5), the cost-effectiveness ratio (C_{DRP}/C_{PV}) consistently exceeds 3.0 across all communities. This indicates that DRP may not be financially superior to a PV-only capacity expansion under current market and incentive assumptions. However, this finding underscores the high non-monetary value of DRP, which provides firm, dispatchable capacity during peak hours or system stress events when PV output may be diminished at peak times and thereby mitigating system damages and protecting socially vulnerable consumers, benefits unavailable from PV alone.

Table 5: Cost-effectiveness comparison of DRP vs. PV capacity across RCMGs. CAPEX: Capital Expenditure.

	Unit	Community 1	Community 2	Community 3
Realized Annual DRP Capacity	kW	1029.1	1150.9	1103.2
Annualized Proxy CAPEX*	$\$/yr$	200	200	200
Annual Operational Cost	$\$/yr$	351.6	377.9	367.3
Total Annual DRP Cost (C_{DRP})	$\$/yr$	206184.9	230558.9	221007.8
Total Annual PV Cost (C_{PV})	$\$/yr$	63225.9	70133.8	68458.7
C_{DRP}/C_{PV}	-	3.26	3.28	3.22

6.3 Economic Benefits

Table (6) presents a summary of economic and environmental benefits under strategy 4. Power sales to households constitute a primary revenue stream for the RCMG owner, with Community 3 yielding the highest annual income at $34,519, followed by Community 2 and 1 at $31,352 and $30,463, respectively. This variation reflects differences in WTP for power supply, which constitutes the primary benefit from the RCMG. Specifically, Community 3 exhibits a higher WTP,

supporting elevated electricity pricing and resulting in greater revenue. In contrast, Community 1 shows a lower WTP and smaller revenue, but the more prominent resilience gains justify the investment. Additionally, sales to the main grid provide supplementary income, ranging from $1,168 to $2,157 annually. Though modest, this shows most power is consumed locally—an essential trait of resilience-oriented MGs.

In terms of operational efficiency and sustainability, notable differences are observed. Community 1 exhibits the highest fuel cost savings (15.03%) and storage utilization (21.0%), reflecting effective coordination between generation units and energy storage operation. Peak supply support remains quite consistent across communities, ranging from 15.29% to 16.60%, indicating uniform relief of stress on critical infrastructure during peak periods. Lastly, a CO_2 abatement via PV (relative to DG-only system with sufficient capacity) of at least 29,000 $kg/year$ underscores the significant environmental contribution of solar generation and the RCMG sustainability. Note that the CO_2 abatement is calculated only for outage hours throughout the year. Collectively, these results reinforce the economic benefits of the RCMG, where strategic storage utilization and fuel displacement play a critical role in shaping both financial performance and environmental benefits.

Table 6: Economic benefits of RCMG under strategy 4.

Benefits	Unit	Community 1	Community 2	Community 3
Power sales to households	$\$/yr$	30,463	31,352	34,519
Power sales to grid	$\$/yr$	1,575	2,157	1,168
Fuel cost savings	%	15.03	13.10	11.73
ES Utilization Rate	%	21	19	13
Peak supply support	%	16.60	16.06	15.29
CO_2 abatement of PV	kg/yr	29,673	28,754	33,921

6.4 RCMG Under Prolonged Outages

We analyze the RCMG scheduling during a high-impact, low-probability outage lasting 152 hours, approximately one week. Figures (7)-(9) illustrate how demand is met by ES, PV, DG, and grid, or otherwise shed, during a week-long outage in August. Peak demand hours occur between 1 PM and 6 PM (13:00–18:00), and the outage begins at 3 PM (15:00), depicted by a dashed line.

The figures underscore the important role of PV and DG in supplying emergency power during

outages. PV units cover the majority of the daytime load (9 AM–6 PM), improving both Λ and E. While there are slight variations in ES utilization, its effective contribution to Φ is evident, particularly in the initial hours of the outage. In Communities 1 and 2, ES is primarily discharged in the evening (after 5 PM) to meet high demand when PV generation ceases. DG also plays a key role in mitigating early outage load loss, thereby strengthening robustness. At night, when PV is inactive and ES has been discharged, DG becomes the sole power source, making its resilience contribution comparable to that of PV. These operational patterns demonstrate a well-coordinated and strategic dispatch of distributed energy resources throughout the day.

Regarding DRP, a noticeable portion of the load is shifted prior to the onset of the outage and during off-peak hours in Community 1 (Figure (10)). A similar pattern is observed in the other communities, as presented in the Appendices. This preemptive shifting enables a significant portion of the load to be served during the first 3-4 hours following the outage, contributing to enhanced robustness. Additionally, by shifting load during off-peak hours, available power resources are preserved to sustain system performance and reliability during peak hours.

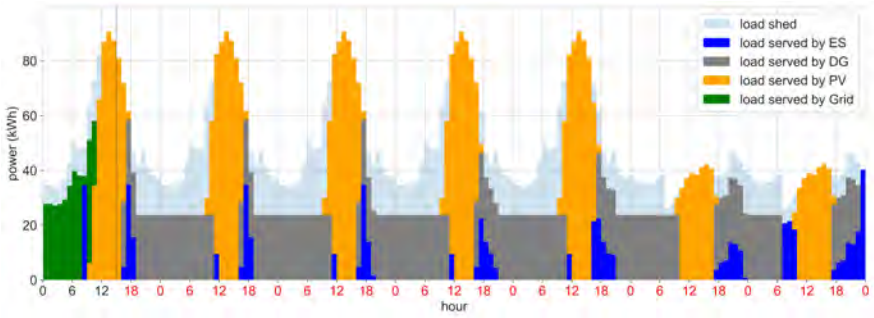

Figure 7: Hourly demand satisfaction in Community 1 during a 152-hour summer outage.

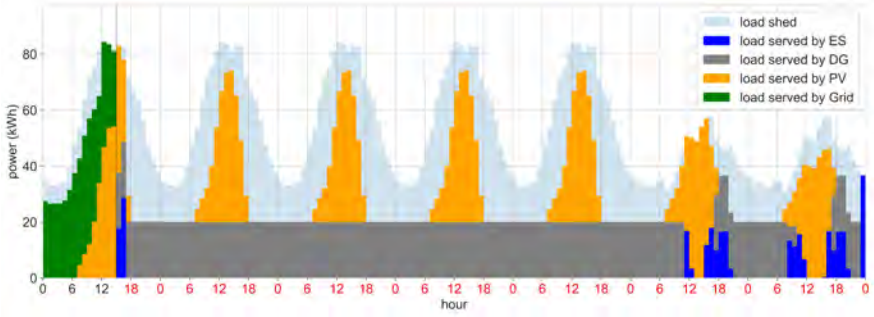

Figure 8: Hourly demand satisfaction in Community 2 during a 152-hour summer outage.

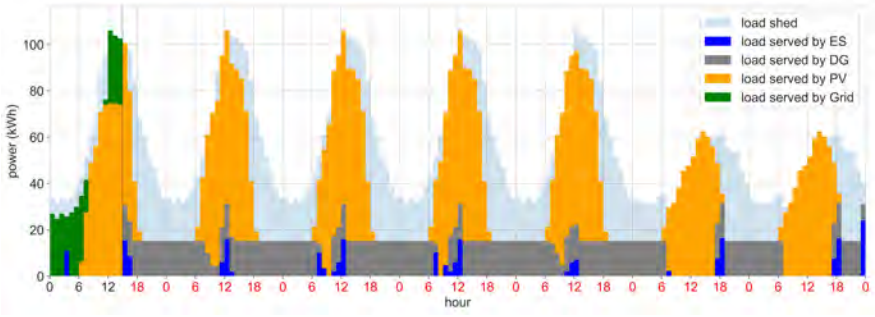

Figure 9: Hourly demand satisfaction in Community 3 during a 152-hour summer outage.

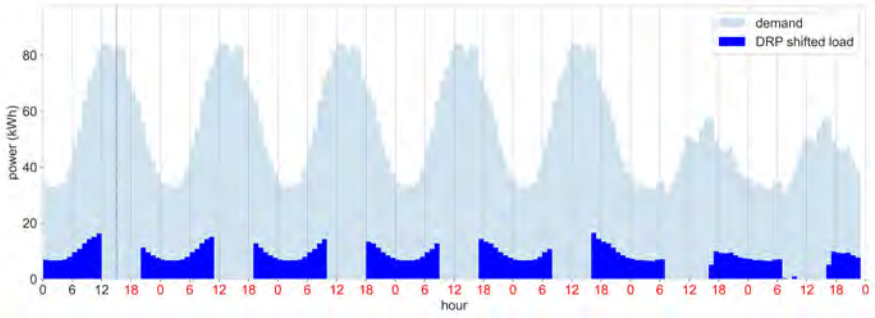

Figure 10: Load curtailment from DRP in Community 1 during a 152-hour summer outage.

6.5 Sensitivity Analysis

This section evaluates the sensitivity of model outcomes to key parameters, including expansion timing, DRP rate, RCMG electricity price, solar generation, and scalability.

6.5.1 Expansion timing

Figure (11) illustrates the changes in investment+expansion costs (denoted as budget), as well as resilience metrics, as the expansion year increases from 4 to 16 in increments of 4. Regardless of the PO-RSVI level, a significant increase in budget is observed when the expansion is delayed to year 12; beyond that point, budget stays the same in Community 1, continues increasing in Community 2, and drops about 2.5% compared to year 12. First, this suggests that delaying expansion leads to larger changes in demand loss in future years. Second, the different budget behavior observed after year 12 indicates that investment decisions are influenced not only by time but also by other community-specific factors that may encourage or discourage further investment.

Figure (11) also shows that delaying expansion leads to either a continuous decline or no improvement in resilience metrics in communities 2 and 3. For Community 1, resilience first improves

at year 8 with Φ undergoing the most improvement and then starts declining till year 16. Even with higher investments between years 8 and 12, resilience continues to decline, likely due to uncertainty in load demand growth.

Regarding bill savings, the sensitivity analysis across selected expansion years (Figure (d) in (11) reveals no substantial benefits from delaying the expansion timeline. While total investment increases with later expansion years, these costs are primarily allocated to support system capacity for outage periods, rather than improving cost efficiency during normal operation. Since bill savings are measured under grid-connected conditions, they reflect the routine economic benefits of the RCMG rather than its resilience performance. The observed increase in investment largely serves to accommodate growing load demand and mitigate the effects of device degradation over time. Therefore, the relatively stable bill savings across different expansion years are justified, as the additional investment supports resilience without directly affecting cost savings.

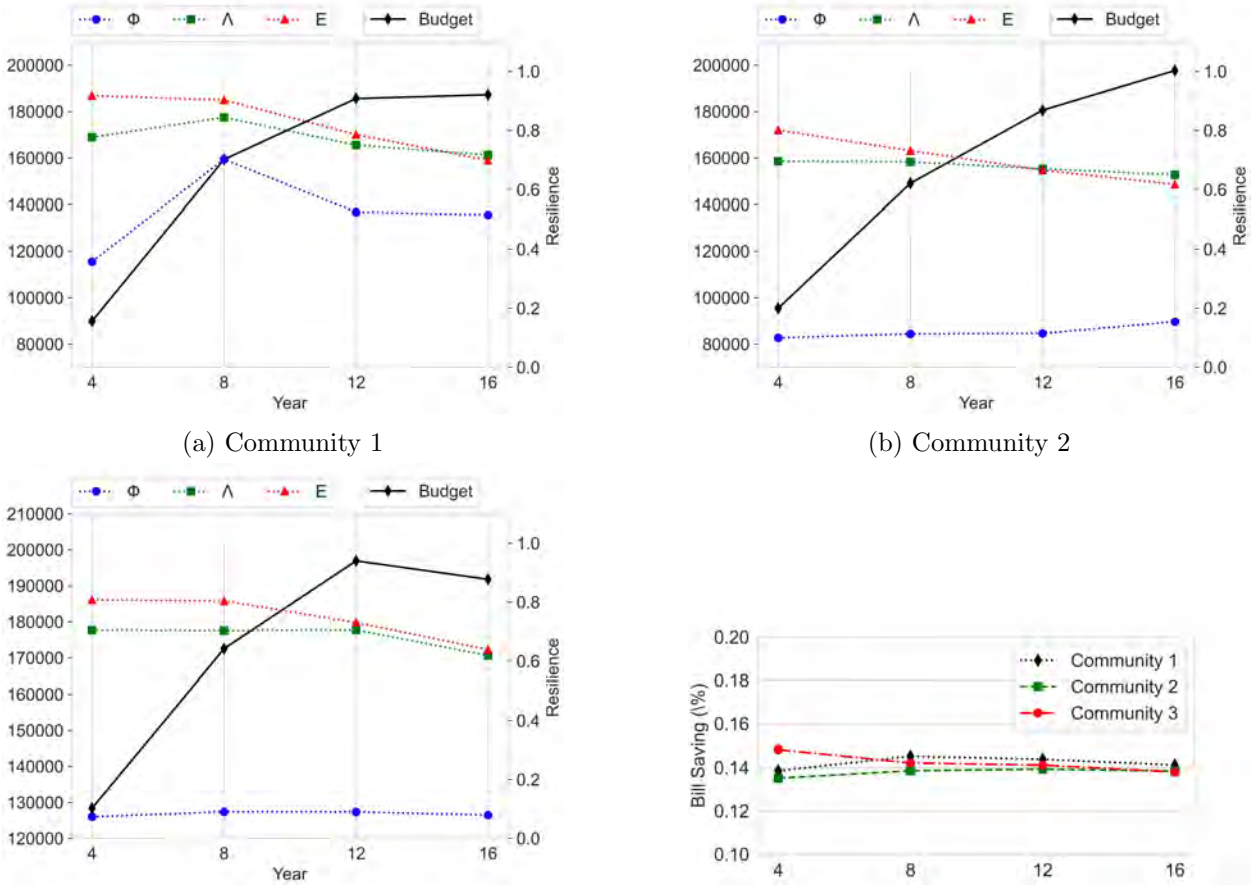

(a) Community 1

(b) Community 2

(c) Community 3

(d) Bill Savings

Figure 11: Sensitivity of investment, resilience, and bill savings to the expansion year.

6.5.2 Rate of DRP

Figure (12) show the sensitivity of budget and resilience to changes in DRP rate (γ^{drp}) ranging from 0.0 to 1.0 in increments of 0.2. Across all communities, higher DRP rates lead to a continuous decline in the allocated budget. These reductions are justified by the role of DRP in alleviating peak demand by curtailing loads, thus reducing the need for additional investment to mitigate load shedding during critical periods. It is important to note that a higher DRP rate does not enforce a fixed amount of load curtailing. Instead, it sets an upper bound, allowing the actual curtailed load to vary dynamically from 0 up to the specified maximum.

In terms of resilience, all communities exhibit either consistent improvements across two metrics Λ and E, with increasing DRP rates. However, the metric Φ demonstrates quite stable behavior. The results indicate that DRP has a smaller impact on robustness but enhances resourcefulness and redundancy, both of which remain beneficial.

Just focusing on bill saving benefits (Figure (d) in (12), we notice steady improvements in all the communities, with steep increases in Community 3, suggesting higher rates with incentives would benefit consumers, encouraging them to participate. However, it is important to recognize that incentives play an important role; without adequate encouragement, higher DRP rates may become less effective or even counterproductive.

6.5.3 RCMG electricity price

Changes in the RCMG-offered electricity price, captured by γ^{l}—the ratio of the power price purchased from the grid—ranging from 0.4 to 1.0 in increments of 0.1, are depicted in Figure (13). While in Community 1, budget remains nearly unchanged with increases in γ^{l}, Communities 2 and 3 are incentivised to install more devices—Community 2 shows a linear increase in investment, whereas Community 3 exhibits exponential growth. In terms of energy resilience, Φ improves only slightly in Community 1, with no observable changes in other metrics across all communities. In communities 2 and 3, higher electricity prices—driven by higher WTP—make larger investments more financially attractive by offering higher revenue potential. However, our analysis indicates that these increased investments do not translate into improved resilience outcomes.

Bill savings associated with each γ^{l}, shown in Figure (d) of (13), indicate that electricity prices

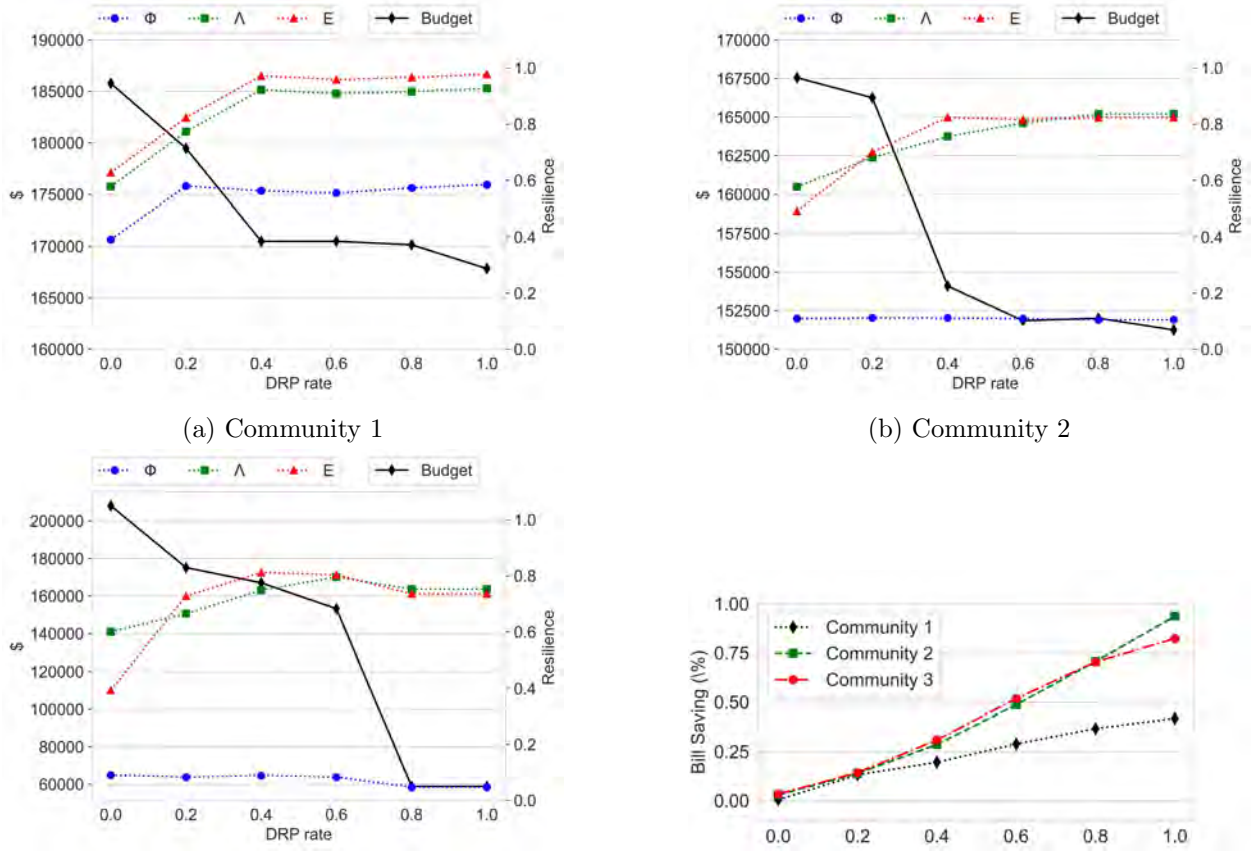

(a) Community 1

(b) Community 2

(c) Community 3

(d) Bill Savings

Figure 12: Sensitivity of investment, resilience, and bill savings to DRP rate.

with $\gamma^l < 0.7$ have little to no impact on bill savings. However, when $\gamma^l \geq 0.7$, bill savings increase by at least 50%, followed by a decline as γ^l approaches 1.0, returning to levels similar to those observed when $\gamma^l < 0.7$. This suggests that setting the RCMG electricity price between 70% and 90% of the grid price yields the highest bill savings for consumers, potentially increasing their willingness to participate.

6.5.4 Solar Power Generation

We evaluate the performance of the RCMG under three solar generation scenarios: baseline, a reduced case with 20% less generation (mostly cloudy days), and an enhanced case with 20% more generation (mostly sunny days). This analysis provides insight into the model's robustness and the sensitivity of investment decisions to changes in solar availability.

Table (7) presents the results of the sensitivity analysis. In addition to capacity decisions,

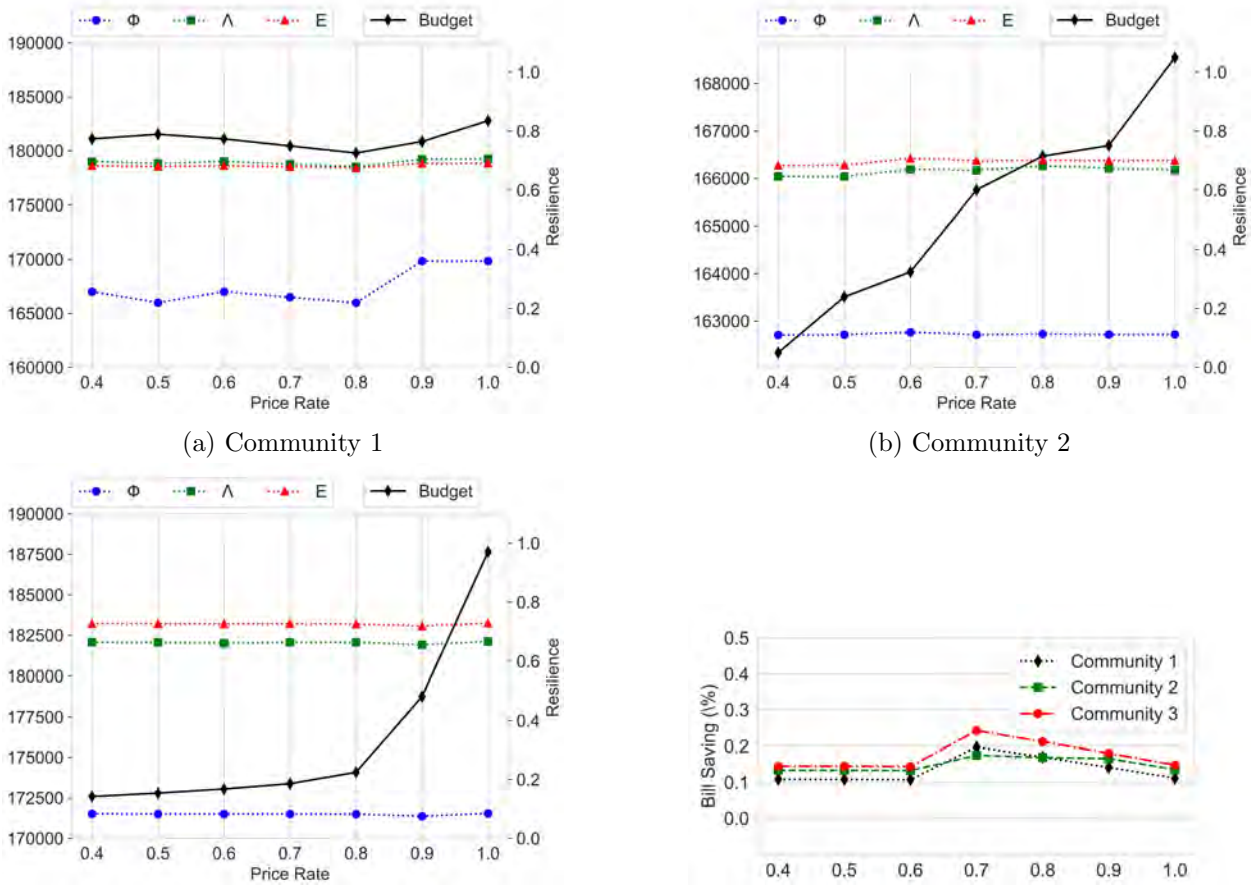

(a) Community 1

(b) Community 2

(c) Community 3

(d) Bill Savings

Figure 13: Sensitivity of investment, resilience, and bill savings to price rate.

investment/expansion costs, and resilience metrics, we report the cost per unit of resilience (CPUR), defined as the total installation cost divided by the percentage resilience score ($100 \times \Phi$), representing the cost of achieving each 1% of robustness. This metric enables assessment of cost-effectiveness in mitigating outage impacts.

In the cloudy scenario, ES capacity decreases across all communities, while PV increases in Community 1 but decreases in Communities 2 and 3. Although one might expect higher PV and ES capacities to compensate for reduced solar generation, the model does not favor additional PV when marginal generation efficiency is low and the cost outweighs the benefit in reducing load shedding. This highlights the complex trade-offs captured by the model, where the optimal combination of PV and ES depends on both solar availability and economic considerations. DG capacity remains unchanged in all communities, as it is constrained by the peak load limit. Resilience declines across

Table 7: Sensitivity analysis to PV generation scenarios.

	Community 1			Community 2			Community 3		
	Cloudy	Base	Sunny	Cloudy	Base	Sunny	Cloudy	Base	Sunny
ES (kW)	61	99	78	46	82	50	41	51	47
PV (kW)	243	220	259	178	185	191	152	176	177
DG (kW)	31	31	31	26	26	26	31	31	31
Investment ($)	105,732	111,725	118,998	106226	112,280	106,226	100,157	128,318	120,273
Expansion (%)	74,242	62,733	75,023	50,591	60,927	61,506	65,420	66,608	72,455
CPUR	5,142	3,115	3,880	14,256	7,531	7,624	27,596	21,658	19,273
Φ	0.35	0.56	0.50	0.11	0.23	0.22	0.06	0.09	0.10
Λ	0.68	0.78	0.74	0.65	0.69	0.70	0.62	0.69	0.71
E	0.67	0.82	0.71	0.67	0.71	0.72	0.70	0.75	0.76

the board in this scenario, with CPUR rising significantly, indicating that reduced PV output makes outages more costly to manage.

In the sunny scenario, PV capacity increases, reflecting both consumer and RCMG owner benefits from higher solar output and the potential to generate revenue by selling excess power. ES on the other hand decreases as higher PV can generate more power to serve the load and avoid loss of power during charge/discharge. Resilience improves across all metrics, and CPUR remains relatively stable, showing that greater solar availability enhances robustness without substantially increasing cost per unit of resilience.

6.5.5 Scalability Analysis and Performance

To evaluate the model's performance under varying community sizes, we scale the case studies by halving and doubling the number of consumers. This scaling is applied to the number of households, energy demand, available space for PV installations, and device capacity limits. Our goal is to assess how community size influences investment decisions and resilience outcomes. Figures (14)-(16) illustrate changes in investment, expansion, and resilience metrics. For clarity, investment and expansion changes are also reported as percentages relative to the baseline (1X) scenario.

According to (a) sub-figures, down-scaling (0.5X) communities leads to 41.9%, 40.0%, and 43.7% reductions in investment for Communities 1, 2, and 3, and 46.6%, 43.1%, and 40.8% reductions in expansion, with the most notable drop in expansion occurring in Community 1. Interestingly, despite being the most vulnerable, Community 1 maintains relatively stable investment while showing the highest drop in expansion, suggesting a focus on core resilience. Under up-scaling (2X),

investment increases by 179.3%, 144.8%, and 135.5%, following the order of vulnerability, whereas expansion increases are more uniform—67.0%, 68.3%, and 69.3%. This contrast indicates that more vulnerable communities prioritize initial investment over expansion, possibly due to the urgency of addressing existing resilience gaps before planning for growth.

Focusing on resilience, a key observation is the consistency of resilience metrics across different community scales, indicating that scaling does not compromise the expected resilience benefits in the proposed framework. This highlights the strength of the methodology in ensuring robust resilience outcomes, even when the model is scaled, as long as demand growth is matched with adequate space and resources for additional installations.

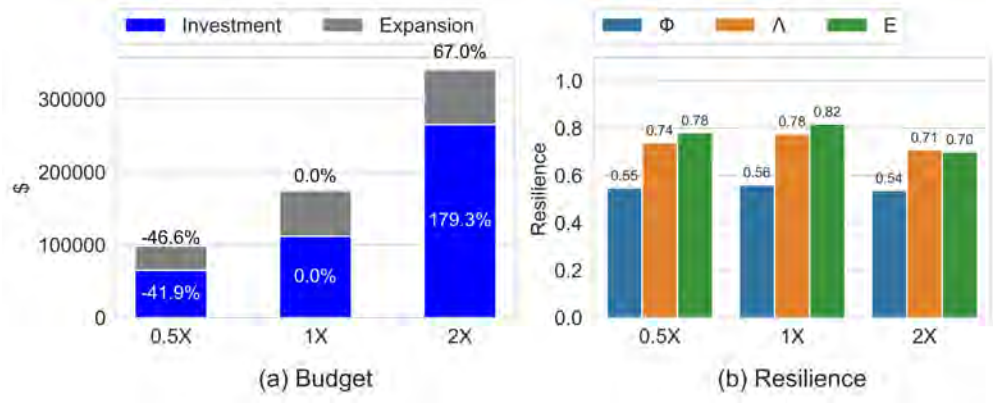

Figure 14: Scalability analysis for Community 1.

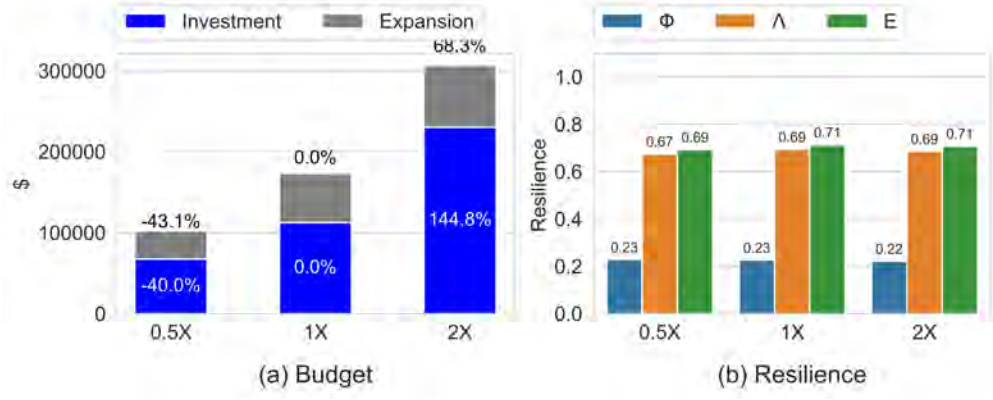

Figure 15: Scalability analysis for Community 2.

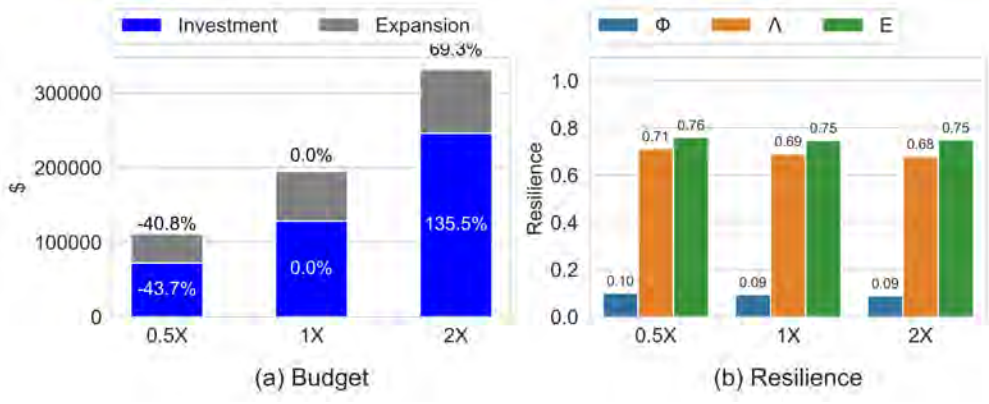

Figure 16: Scalability analysis for Community 3.

7 Discussion

This section provides a detailed evaluation of cost, resilience, and equity outcomes to guide stakeholders—including investors, utilities, and policymakers—in making informed decisions on RCMG planning and implementation.

7.1 Costs, Resilience, and Equity Outcomes

Building on the RCMG analysis, we discuss how expansion timing, DRP design, electricity pricing, and community scale influence cost, resilience, and equity, highlighting practical implications for investors, utilities, and policymakers.

Investment Costs: Timely expansion reduces initial RCMG investment costs by over 15% in highly vulnerable communities, while delaying capacity additions beyond year 4 increases costs without proportional benefits. When expansion is combined with DRP at ratio 20% , it achieves up to 30% investment savings. This finding is consistent with recent studies, which show that incorporating DRP into microgrid operation improves economic efficiency by reducing generation costs and limiting the need for over-sized capacity during peak demand periods [60]. Our model shows when electricity pricing is set at 70–90% of grid tariffs, investment is incentivized by higher expected revenues. While this specific threshold is unique to our study, related work supports the mechanism that cost-reflective tariffs boost DER adoption [61]. This aligns with our result that tariff signals are key to triggering investment in communities with higher WTP.

Energy Resilience: DRP with ratio of 20% enhances resilience metrics, including robustness,

resourcefulness, and redundancy, by enabling flexible, incentivized load curtailment, and better use of existing capacity. Expansion timing ensures sufficient capacity during outages and when integrated with DRP it yields the highest resilience scores. The week-long outage analysis shows how PV meets daytime loads, ES covers evening peaks, and DG supports night-time demand, together sustaining resilience metrics. Preemptive DRP shifts reduce early load shedding and preserve ES and DG capacity for critical hours. Coordinated dispatch across these resources maintains continuity throughout the outage, with observed patterns consistent with prior studies [16], while also highlights potential bottlenecks in storage and DG capacity for long-duration resilience.

Equity: DRP and expansion strategies generate household bill savings of 12–13% (approximately $300 annually), providing tangible benefits for vulnerable populations. Higher DRP rates also provide financial incentives, encouraging broader consumer participation. These findings are consistent with prior studies demonstrating that community microgrids and integrated energy management strategies deliver both financial relief and reliable service to vulnerable populations [17, 54]. Equity can be enhanced further through targeted subsidies, performance-based incentives, and education programs, ensuring that microgrid deployment delivers both operational and financial relief.

7.2 Managerial & Policy Implications for Cost, Resilience, and Equity

Findings from this study provide the following policy recommendations to guide cost-resilience-equity promoted RCMG planning and implementation.

Economic Drivers: The economic analysis demonstrates clear implications for both cost and equity, as well as investment decisions. Investors benefit primarily from local power sales, with communities showing higher WTP offering greater financial returns and stronger justification for investments. In lower-WTP communities investment is discouraged due to limited revenue potential. Policymakers can address this imbalance by providing targeted incentives such as capital subsidies, performance-based grants, or favorable financing mechanisms, ensuring that investments deliver both financial viability and equitable access to resilient energy. Promoting consumer participation through education and equitable tariff design can further enhance WTP and long-term project viability. Observed fuel savings and CO_2 reductions also highlight opportunities to align cost-efficiency with resilience and sustainability objectives, consistent with findings in the literature [62].

Operation Under Prolonged Outages: The week-long outage analysis highlights the important role of resilience in maintaining power supply. Diversified and strategically dispatched energy resources, combined with preemptive DRP and advanced control systems, reduce load shedding and maintain continuity during extreme events. For utilities, this translates into operational cost savings and more reliable service. For policymakers, supporting frameworks that prioritize resilience alongside economic efficiency ensures that vulnerable communities maintain service continuity, supporting both equity and system reliability.

Impact of Solar Variability: Variable solar generation affects the cost-resilience trade-off. For policymakers, reduced solar availability significantly increases the cost per unit of resilience (CPUR), highlighting the importance of targeted subsidies or performance-based incentives to sustain resilience in less favorable conditions. Utilities should integrate climate-adjusted solar forecasts into planning to anticipate future cost-resilience trade-offs and adjust procurement strategies accordingly. In high-solar scenarios, stable CPUR and increased resilience suggest that maximizing solar uptake through favorable tariffs or streamlined interconnection processes can provide cost-effective gains, improve robustness, and deliver consumer savings, supporting both economic efficiency and equitable access to resilient energy, consistent with findings in the literature [16, 63].

Scaling Microgrid Design for Community Size: When scaling RCMG to larger communities, resilience can be maintained if additional DER installations match growth in demand. Proactive planning—including permitting, zoning flexibility, and early-stage incentives—ensures cost-effective expansion and equitable access to energy services. In vulnerable communities, front-loaded funding programs or resilience grants can address immediate infrastructure needs without compromising long-term scalability, supporting both equity and cost-efficiency.

8 Conclusion

In this study, we proposed a RCMG planning and operation framework to enhance energy resilience in socially vulnerable communities. The RCMG is formulated as a two-stage stochastic program minimizing investment, expansion, and week-based operational costs over a 20-year horizon. A load-curtailing DRP is introduced to shift demand from peak to off-peak hours, mitigating outage impacts while offering bill discounts to participating households. Three resilience metrics, Φ, Λ,

and E, evaluate robustness, resourcefulness, and redundancy. Extensive numerical analyses provide operational and managerial insights to support resilient energy system design.

Results show that combining capacity expansion with DRP yields the most promising outcomes—reducing costs up to 16%, enhancing resilience up to 60%, and providing bill savings up to 13%. DRP design significantly influences the balance between cost efficiency and resilience, while timely expansion prevents ineffective spending. Electricity pricing affects financial accessibility and investment behavior without undermining resilience, highlighting the value of calibrated price signals within 70–90% of grid prices. Aligning economic incentives with resilience goals is key to effective microgrid deployment, guiding policymakers toward equitable and scalable planning, and supporting utilities and investors in adaptive, coordinated strategies for robust energy systems.

This study provides a foundation for future work to extend the framework to other states in the U.S., integrate additional renewable sources (e.g., wind, geothermal), and account for longer outages and evolving community conditions through a dynamic PO-RSVI. Future research could also incorporate real-time operational dynamics such as ESS degradation, differentiate outage causes, and evaluate broader economic impacts. Expanding to peer-to-peer energy sharing, dynamic grid-islanded operations, and detailed cost-benefit and incentive analyses can further support equitable and resilient energy planning while exploring Pareto-optimal trade-offs among cost, resilience, and equity.

9 Data and Code Availability

For the code and data used in the study visit the GitHub repository github.com/FarzaneEzzati/RCMG-PlanningOperation.

10 Acknowledgment

The authors gratefully acknowledge the financial support of the U.S. Department of Energy Solar Energy Technologies Office under the Science and Technology Research Partnership (STRP). They also extend their sincere appreciation to the Sunnyside Community in Houston, TX, and the Rogers Washington and Dove Springs Communities in Austin, TX, for their invaluable input to this study.

References

[1] DOE DoE. Electric Disturbance Events (OE-417) Annual Summaries. 2023.

[2] Central C. Weather-related Power Outages Rising; 2024. Available from: https://www.climatecentral.org/climate-matters/weather-related-power-outages-rising.

[3] Express-News SA. Texas Has Had the Most Power Outages Over Past 5 Years; 2024. Available from: https://www.governing.com/infrastructure/texas-has-had-the-most-power-outages-over-past-5-years.

[4] Abdin AF, Fang YP, Zio E. A modeling and optimization framework for power systems design with operational flexibility and resilience against extreme heat waves and drought events. Renewable and Sustainable Energy Reviews. 2019;112:706-19.

[5] Panteli M, Trakas DN, Mancarella P, Hatziargyriou ND. Power systems resilience assessment: Hardening and smart operational enhancement strategies. Proceedings of the IEEE. 2017;105(7):1202-13.

[6] Fang YP, Zio E. An adaptive robust framework for the optimization of the resilience of interdependent infrastructures under natural hazards. European Journal of Operational Research. 2019;276(3):1119-36.

[7] Mohamed MA, Chen T, Su W, Jin T. Proactive resilience of power systems against natural disasters: A literature review. IEEE Access. 2019;7:163778-95.

[8] Molavi A, Shi J, Wu Y, Lim GJ. Enabling smart ports through the integration of microgrids: A two-stage stochastic programming approach. Applied Energy. 2020;258:114022.

[9] Hamidieh M, Ghassemi M. Microgrids and resilience: A review. IEEE Access. 2022;10:106059-80.

[10] Uddin M, Mo H, Dong D, Elsawah S, Zhu J, Guerrero JM. Microgrids: A review, outstanding issues and future trends. Energy Strategy Reviews. 2023;49:101127.

[11] Miao L, Zhou N, Ma J, Liu H, Zhao J, Wei X, et al. Current Status, Challenges and Future Perspectives of Operation Optimization, Power Prediction and Virtual Synchronous Generator of Microgrids: A Comprehensive Review. Energies. 2025;18(13):3557.

[12] Bokkisam HR, Singh S, Acharya RM, Selvan MP. Blockchain-based peer-to-peer transactive energy system for community microgrid with demand response management. CSEE Journal of Power and Energy Systems. 2021;8(1):198-211.

[13] Alilou M, Tousi B, Shayeghi H. Home energy management in a residential smart micro grid under stochastic penetration of solar panels and electric vehicles. Solar Energy. 2020;212:6-18.

[14] Moradi M, Farzaneh H. Demand response programs in decentralized hybrid local energy markets: Evaluating the impact of risk-adjusted behavior of market players and the integration of renewable energy sources, using a novel bi-level optimization framework. Applied Energy. 2025;390:125806.

[15] de Lima TD, Lezama F, Soares J, Franco JF, Vale Z. Modern distribution system expansion planning considering new market designs: Review and future directions. Renewable and Sustainable Energy Reviews. 2024;202:114709.

[16] Chowdhury T, Chowdhury H, Islam KS, Sharifi A, Corkish R, Sait SM. Resilience analysis of a PV/battery system of health care centres in Rohingya refugee camp. Energy. 2023;263:125634.

[17] Sabzi B, Shi J, Lim G, Ezzati F, Wang K. Energy equity-centered planning of community microgrids. Sustainable Cities and Society. 2025:106485.

[18] Islam KS, Hasan S, Chowdhury T, Chowdhury H, Sait SM. Outage survivability investigation of a PV/battery/CHP system in a hospital building in Texas. sustainability. 2022;14(22):14965.

[19] Adger WN. Vulnerability. Global environmental change. 2006;16(3):268-81.

[20] Dugan J, Byles D, Mohagheghi S. Social vulnerability to long-duration power outages. International Journal of Disaster Risk Reduction. 2023;85:103501.

[21] Ezzati F, Xiao Q, Dong ZS, Jiao J, Vargas A, Yeh V, et al. Power outage-risk integrated social vulnerability analysis highlights disparities in small residential communities. Communications Earth & Environment. 2025;6(1):294.

[22] Hensher DA, Shore N, Train K. Willingness to pay for residential electricity supply quality and reliability. Applied energy. 2014;115:280-92.

[23] Mishra S, Anderson K, Miller B, Boyer K, Warren A. Microgrid resilience: A holistic approach for assessing threats, identifying vulnerabilities, and designing corresponding mitigation strategies. Applied Energy. 2020;264:114726.

[24] Ezzati F, Lim G, Dong ZS. Equitable Energy Trading in Microgrids to Enhance Resilience and Cost Efficiency. In: 2025 IEEE International Communications Energy Conference (INTELEC); 2025. p. 49-54.

[25] Singh V, Moger T, Jena D. Uncertainty handling techniques in power systems: A critical review. Electric Power Systems Research. 2022;203:107633.

[26] Rajamand S. Effect of demand response program of loads in cost optimization of microgrid considering uncertain parameters in PV/WT, market price and load demand. Energy. 2020;194:116917.

[27] Wang F, Ge X, Yang P, Li K, Mi Z, Siano P, et al. Day-ahead optimal bidding and scheduling strategies for DER aggregator considering responsive uncertainty under real-time pricing. Energy. 2020;213:118765.

[28] Thang VV, Ha T, Li Q, Zhang Y. Stochastic optimization in multi-energy hub system operation considering solar energy resource and demand response. International Journal of Electrical Power & Energy Systems. 2022;141:108132.

[29] Khayatian A, Barati M, Lim GJ. Integrated microgrid expansion planning in electricity market with uncertainty. IEEE Transactions on Power Systems. 2017;33(4):3634-43.

[30] Dong J, Zhu L, Su Y, Ma Y, Liu Y, Wang F, et al. Battery and backup generator sizing for a resilient microgrid under stochastic extreme events. IET Generation, Transmission & Distribution. 2018;12(20):4443-50.

[31] Yang H, Nagarajan H. Optimal power flow in distribution networks under N–1 disruptions: A multistage stochastic programming approach. INFORMS Journal on Computing. 2022;34(2):690-709.

[32] Lee J, Lee Sg, Lee K. Multistage Stochastic Optimization for Microgrid Operation Under Islanding Uncertainty. IEEE Transactions on Smart Grid. 2021;12.

[33] Boloukat MHS, Foroud AA. Stochastic-based resource expansion planning for a grid-connected microgrid using interval linear programming. Energy. 2016;113:776-87.

[34] Wei Z, Yang L, Chen S, Ma Z, Zang H, Fei Y. A multi-stage planning model for transitioning to low-carbon integrated electric power and natural gas systems. Energy. 2022;254:124361.

[35] Varasteh F, Nazar MS, Heidari A, Shafie-khah M, Catalão JPS. Distributed energy resource and network expansion planning of a CCHP based active microgrid considering demand response programs. Energy. 2019;172:79-105.

[36] Mehrjerdi H. Dynamic and multi-stage capacity expansion planning in microgrid integrated with electric vehicle charging station. Journal of Energy Storage. 2020;29:101351.

[37] Pecenak ZK, Stadler M, Fahy K. Efficient multi-year economic energy planning in microgrids. Applied Energy. 2019;255:113771.

[38] Fioriti D, Poli D, Duenas-Martinez P, Perez-Arriaga I. Multi-year stochastic planning of off-grid microgrids subject to significant load growth uncertainty: overcoming single-year methodologies. Electric Power Systems Research. 2021;194:107053.

[39] Pang K, Zhou J, Tsianikas S, Coit DW, Ma Y. Long-term microgrid expansion planning with resilience and environmental benefits using deep reinforcement learning. Renewable and Sustainable Energy Reviews. 2024;191:114068.

[40] Li Y, Wang J, Zhou Y, Wei C, Guan Z, Chen H. Multi-dimension day-ahead scheduling optimization of a community-scale solar-driven CCHP system with demand-side management. Renewable and Sustainable Energy Reviews. 2023;185:113654.

[41] Rasoulinezhad H, Abapour M, Sadeghian O, Zare K. The role of risk-based demand response in resource management of a grid-connected renewable-based large-scale microgrid with stationary and mobile energy storage systems and emission tax. Computers & Industrial Engineering. 2023;183:109555.

[42] Zhang W, Valencia A, Gu L, Zheng QP, Chang N. Integrating emerging and existing renewable energy technologies into a community-scale microgrid in an energy-water nexus for resilience improvement. Applied Energy. 2020;279:115716.

[43] Hai T, Zhou J, Rezvani A, Le BN, Oikawa H. Optimal energy management strategy for a renewable based microgrid with electric vehicles and demand response program. Electric Power Systems Research. 2023;221:109370.

[44] Basu M. Optimal generation scheduling of hydrothermal system with demand side management considering uncertainty and outage of renewable energy sources. Renewable Energy. 2020;146:530-42.

[45] Mansouri SA, Ahmarinejad A, Javadi MS, Catalão JPS. Two-stage stochastic framework for energy hubs planning considering demand response programs. Energy. 2020;206:118124.

[46] Vahedipour-Dahraie M, Rashidizadeh-Kermani H, Anvari-Moghaddam A. Risk-based stochastic scheduling of resilient microgrids considering demand response programs. IEEE Systems Journal. 2020;15(1):971-80.

[47] Raghav LP, Kumar RS, Raju DK, Singh AR. Analytic hierarchy process (AHP)–swarm intelligence based flexible demand response management of grid-connected microgrid. Applied energy. 2022;306:118058.

[48] Habib HUR, Waqar Ad, Hussien MG, Junejo AK, Jahangiri M, Imran RM, et al. Analysis of microgrid's operation integrated to renewable energy and electric vehicles in view of multiple demand response programs. IEEE Access. 2022;10:7598-638.

[49] Yang Z, Tian H, Min H, Yang F, Hu W, Su L, et al. Optimal microgrid programming based on an energy storage system, price-based demand response, and distributed renewable energy resources. Utilities Policy. 2023;80:101482.

[50] Tamasiga P, Onyeaka H, Altaghlibi M, Bakwena M, houssin Ouassou E. Empowering communities beyond wires: Renewable energy microgrids and the impacts on energy poverty and socio-economic outcomes. Energy Reports. 2024;12:4475-88.

[51] Geoffrion AM, Graves GW. Multicommodity distribution system design by Benders decomposition. Management science. 1974;20(5):822-44.

[52] Bruneau M, Chang SE, Eguchi RT, Lee GC, O'Rourke TD, Reinhorn AM, et al. A framework to quantitatively assess and enhance the seismic resilience of communities. Earthquake spectra. 2003;19(4):733-52.

[53] Panteli M, Mancarella P, Trakas DN, Kyriakides E, Hatziargyriou ND. Metrics and quantification of operational and infrastructure resilience in power systems. IEEE Transactions on Power Systems. 2017;32(6):4732-42.

[54] Anderson K, Burman K, Simpkins T, Helson E, Lisell L. New York solar smart DG hub-resilient solar project: Economic and resiliency impact of PV and storage on New York critical infrastructure. National Renewable Energy Lab.(NREL), Golden, CO (United States); 2016.

[55] Wood E, Sanders M, Frazier T. The practical use of social vulnerability indicators in disaster management. International Journal of Disaster Risk Reduction. 2021;63:102464.

[56] Hotaling C, Bird S, Heintzelman MD. Willingness to pay for microgrids to enhance community resilience. Energy Policy. 2021;154:112248.

[57] Wilson E, Parker A, Fontanini A, Present. End-Use Load Profiles for the U.S. Building Stock. 2021 10.

[58] EIA USEIA. Residential Sector Energy Consumption Estimates, 1960-2021, Texas http://www.eia.gov/state/seds/. 2023.

[59] Piette MA, Schetrit O, Kiliccote S, Cheung I, Li BZ. Costs to automate demand response-taxonomy and results from field studies and programs. 2015.

[60] Dey B, Misra S, Marquez FPG. Microgrid system energy management with demand response program for clean and economical operation. Applied Energy. 2023;334:120717.

[61] Spiller E, Esparza R, Mohlin K, Tapia-Ahumada K, Ünel B. The role of electricity tariff design in distributed energy resource deployment. Energy Economics. 2023;120:106500.

[62] Chowdhury T, Chowdhury H, Miskat MI, Chowdhury P, Sait SM, Thirugnanasambandam M, et al. Developing and evaluating a stand-alone hybrid energy system for Rohingya refugee community in Bangladesh. Energy. 2020;191:116568.

[63] Chowdhury H, Chowdhury T, Rahman MS, Masrur H, Senjyu T. A simulation study of techno-economics and resilience of the solar PV irrigation system against grid outages. Environmental Science and Pollution Research. 2022;29(43):64846-57.